Sónia Cristina Pereira Marques

Licenciada em Ciências da Engenharia Química e Bioquímica

EDIBLE COATINGS BASED ON CHITOSAN-BEESWAX EMULSIONS

Dissertação para obtenção do Grau de Mestre em Engenharia Química e Bioquímica

Orientador: Isabel Maria Rôla Coelhoso, Professora Doutora, FCT/UNL
Co-orientador: Vítor Manuel Delgado Alves, Professor Doutor, ISA/UTL

Júri:

Presidente: Prof. Doutora Maria da Ascensão Carvalho Fernandes Miranda Reis
Arguente: Prof. Doutora Margarida Mendes Moldão-Martins
Vogais: Prof. Doutora Isabel Maria Rôla Coelhoso
Prof. Doutor Vítor Manuel Delgado Alves

FACULDADE DE CIÊNCIAS E TECNOLOGIA
UNIVERSIDADE NOVA DE LISBOA

Outubro 2012

Sónia Cristina Pereira Marques

Licenciada em Ciências da Engenharia Química e Bioquímica

EDIBLE COATINGS BASED ON CHITOSAN-BEESWAX EMULSIONS

Dissertação apresentada à Faculdade de Ciências e Tecnologia da Universidade Nova de Lisboa para obtenção do Grau de Mestre em Engenharia Química e Bioquímica

Outubro 2012

EDIBLE COATINGS BASED ON CHITOSAN-BEESWAX EMULSIONS

AGRADECIMENTOS

Gostaria de agradecer em primeiro lugar à Rita Ferreira pela sua transmissão de conhecimentos, explicações e demonstrações e também pela sua partilha de experiencias que muito me ajudaram e foram essenciais para a realização deste trabalho. Por toda a sua simpatia e por sempre falar comigo com um sorrido na cara mesmo quando estava cansada ou quando o seu trabalho não corria tão bem.

Agradeço também aos meus orientadores, Isabel Coelhoso e Vítor Alves pelo entusiasmo demostrado na escolha do tema, pela motivação que me transmitiram ao longo deste trabalho, pelas explicações e esclarecimento de dúvidas que foram surgindo e também pela simpatia com que sempre me trataram.

Ao Diogo por toda a paciência que teve comigo, pelo amor e carinho e pelo apoio que me deu mesmo nos momentos mais difíceis, sem ele teria sido muito mais difícil: obrigada por tudo! Também aos pais e irmã do Diogo que têm sido para mim uma segunda família: obrigada por sempre me terem tratado tão bem e por gostarem tanto de mim!

Aos amigos e colegas que estiveram comigo ao longo desta etapa e que directa ou indirectamente contribuíram para que eu chegasse até aqui. Agradeço em especial à Catarina Silva que se revelou uma grande amiga e excelente companhia, que com as suas histórias foi sempre capaz de me animar e muito me motivou e incentivou: agora será a tua vez, sabes que podes sempre contar comigo!

A todo o pessoal do laboratório que tão bem me acolheu, em especial à Rute Ferreira que com todo o seu bom humor e boa disposição foi uma óptima colega de bancada.

Por fim mas não menos importante, agradeço aos meus pais por todo o amor, carinho e apoio. Pela paciência que tiveram que ter nos dias maus: já sabem que acabamos sempre por tratar pior as pessoas de quem mais gostamos! Agradeço por sempre terem feito questão que tirasse o curso e por nunca se terem arrependido do esforço, que sei que foi muito grande, por sempre me terem dado as melhores condições e nunca terem deixado que nada me faltasse. Um obrigado muito especial à minha mãe pelo seu grande exemplo de força: amo-te muito!

ABSTRACT

The use of edible biopolymer-based films and coatings is an environmentally friendly technology that offers substantial advantages for increase of shelf-life of many food products including fruits and vegetables. The development of this kind of films and coatings is a technological challenge for the industry and a very active research field worldwide.

In this work biodegradable edible films of chitosan with different contents of beeswax were prepared and characterized. Their hygroscopic properties and water vapour permeability, as well as their CO_2 and O_2 permeability, mechanical, optical and superficial properties were determined.

All the obtained films are transparent with a slightly yellowish colour. They are homogeneous and dense, despite the films with beeswax presented some cracks and depressions in their structure. The incorporation of beeswax increases the films hydrophobicity, higher contact angle values, but still prevails their hydrophilic nature.

Regarding the mechanical properties, these films are flexible and elastic, but the increase of beeswax content increases their brittleness.

The films showed decreased water vapour permeability as well as decreased hydrophilic properties, with the increase of beeswax content. The sorption and diffusion coefficients were evaluated for water vapour transport. The permeability decrease was mainly due to the reduction of the diffusion coefficient. A reduction of the water vapour permeability and a significant reduction in oxygen permeability were achieved with the inclusion of beeswax in the polymeric matrix. Comparing to the films without beeswax, the water vapour permeability decreased 32% and the oxygen permeability 90% for the films with 10% beeswax. Regarding the carbon dioxide permeability, it increased about 240% for the films with 10% beeswax.

From the results, it is thought that these films are promising to be used in food packaging mainly for fruits and vegetable coating, mainly due to their barrier properties that allow the products to breathe and inhibit the oxidation process.

Keywords: *Edible films and coatings; Chitosan films; Beeswax emulsions; Barrier properties*

RESUMO

O uso de filmes e revestimentos comestíveis produzidos a partir de biopolímeros é uma tecnologia amiga do ambiente que oferece vantagens substanciais no aumento do tempo de vida útil de muitos produtos alimentares incluindo frutos e vegetais. O desenvolvimento deste tipo de filmes e revestimentos é um desafio tecnológico para a indústria e um campo de pesquisa e investigação muito activo universalmente.

Neste trabalho, foram preparados e caracterizados filmes comestíveis e biodegradáveis de quitosano com diferentes conteúdos de cera de abelhas. As suas propriedades higroscópicas e permeabilidade ao vapor de água assim como permeabilidade ao CO_2 e O_2, propriedades mecânicas, ópticas e superficiais foram determinadas.

Todos os filmes obtidos são transparentes com uma ligeira tonalidade amarela. Os filmes são homogéneos, densos e sem poros apesar dos filmes com cera apresentarem algumas fissuras e depressões na sua estrutura. A incorporação de cera aumenta a hidrofobia e os valores do angulo de contacto mas a sua natureza hidrofílica prevalece.

No que diz respeito às propriedades mecânicas, estes filmes são flexíveis e elásticos mas o aumento da percentagem de cera incorporada aumenta também a sua fragilidade.

Os filmes mostraram uma diminuição na permeabilidade ao vapor de água assim como uma diminuição nas propriedades hidrofílicas com o aumento do conteúdo de cera. Os coeficientes de solubilidade e difusão foram avaliados para o transporte de vapor de água. A diminuição da permeabilidade deve-se principalmente à redução do coeficiente de difusão. Uma redução na permeabilidade ao vapor de água e uma significante redução na permeabilidade ao oxigénio foram conseguidas com a inserção de cera de abelhas na matriz polimérica. Comparando com os filmes sem cera, a permeabilidade ao vapor de água diminuiu 32% e a permeabilidade ao oxigénio cerca de 90% para os filmes com 10% de cera de abelhas. No que diz respeito à permeabilidade ao dióxido de carbono, esta aumentou cerca de 240% para os filmes com 10% de cera.

A partir dos resultados obtidos, considera-se que estes filmes são promissores no que diz respeito ao seu uso como revestimentos alimentares principalmente para frutos e legumes, principalmente devido às suas propriedades barreira que permitem que os produtos façam a respiração mas inibem o processo de oxidação.

Palavras-chave: *Filmes e revestimentos comestíveis; Filmes de Quitosano; Emulsões com cera de abelhas; Propriedades barreira.*

TABLE OF CONTENTS

INDEX OF FIGURES

INDEX OF TABLES

1 INTRODUCTION

1.1 BACKGROUND

The quality of food products depends on its organoleptic, nutritional and microbiological properties, which are subjected to dynamic alterations during its storage and distribution. These alterations are mainly due to the interactions between the food and the surrounding environment. [1] [2]

The food packaging material is an important factor in the food industry and it's dominated by petroleum-based polymers. Nevertheless, the research involving the production and characterization of edible biodegradable films has grown considerably, mainly due to the interest in minimizing the ecological impact caused by the use of synthetic non-biodegradable packaging materials. [3]

In the last decade, a considerable amount of work focused on the development of films and coatings based on proteins and polysaccharides with food additives from natural or synthetic sources to control microbial growth on fresh and processed foods has emerged. [4] However, the hydrophilic character of these compounds limits its capacity of providing the desired mechanical and functional properties to the edible films. [5]

More recent approaches to improve the mechanical and functional properties of such films include:

- → Incorporation of hydrophobic compounds such as lipids to improve their resistance to water;
- → Optimization of the interaction between polymers (protein-protein interactions, charge-charge electrostatic complexes between proteins or polysaccharides);
- → Cross-linking or functionalization through physical, chemical or enzymatic treatments. [5]

Within the polysaccharides, chitosan offers real potential applications in the food industry due to its particular physicochemical properties, short time biodegradability, biocompatibility with human tissues, antimicrobial and antifungal activities, and non-toxicity. [6] It is a biopolymer produced from a renewable source, derived from a byproduct of the seafood industry, making its use environmentally friendly. [3] In addition to the research based on its antimicrobial properties, some aspects such as mechanical and thermal properties and permeability to gases (O_2, CO_2) have been quantified, revealing that chitosan films plasticized with polyols suffer an increase in permeability as the amount of plasticizers in their formulation is increased. [7]

1.2 OBJECTIVES AND MOTIVATION

This thesis aimed at the preparation of biodegradable edible coatings from chitosan and chitosan-beeswax mixtures. In order to characterize them, the coatings were produced in the form of films. The formulation of the chitosan films was made according to an already existent protocol and the chitosan-beeswax emulsions were optimized in the beginning of this work.

The characterization of the films was based in the study of the optical properties of transparency and colour alteration that the films can induce on surfaces as well as the superficial properties represented by the contact angle determination. Structural properties were studied trough scanning electron microscopy (SEM) were essentially the films without beeswax was compared to the ones with beeswax incorporated.

Thereafter, the hygroscopic properties were studied and the water sorption isotherm for every film was obtained. The solubility and swelling of the films in water was not determined due to its strong hydrophilicity.

Mechanical properties are essential and one of the most important characteristics of the edible biopolymer-based films so they were studied and analysed throughout this work. Not less important are the barrier properties that can help making the choice between different food coatings, so the water vapour, carbon dioxide and oxygen permeability were determined and analysed.

This work, as well as other works with the same objectives, is of extreme importance for the food industry, sustainability, reduction and reuse of natural wastes as substitutes of plastics and synthetic polymers in the food industry.

2 LITERATURE REVIEW

2.1 EDIBLE FILMS

Concerns on environmental waste problems caused by non-biodegradable petrochemical-based plastic packaging materials as well as the consumer's demand for high quality food products has caused an increasing interest in developing biodegradable packaging materials using natural biopolymers such as polysaccharides and proteins. [2]

When a packaging material such as a film or a coating is an integral part of a food and is eaten with the food, it qualifies as "edible" packaging. Coatings are either applied or formed directly on foods, while films, on the other hand, are self-supporting structures that can be used to wrap food products. They are located either on the food surface or as thin layers between different components of a food product. An example of the latter would be a film placed between the fruit and the dough in a pie to provide protection against transfer and mechanical stress (Figure 2.1). [1]

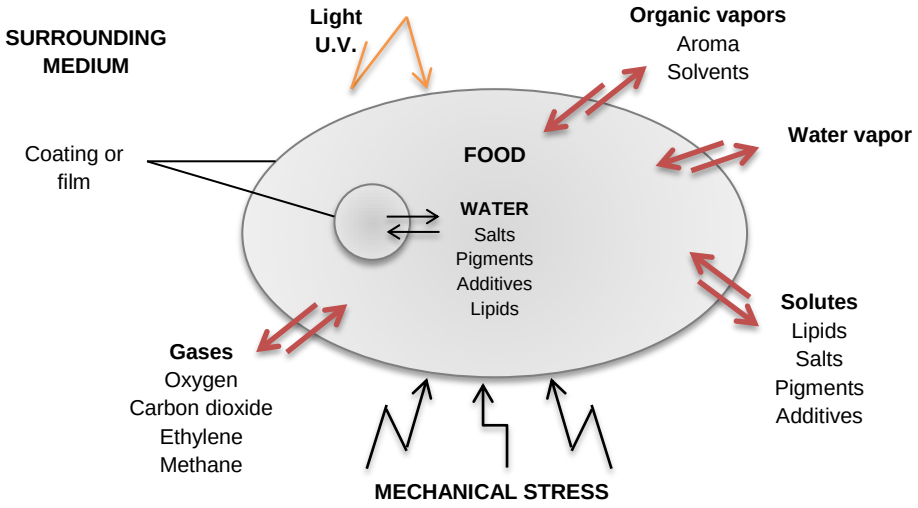

Figure 2.1 – Transfers that can be potentially controlled by edible barriers (Adapted from [1]).

The envelope (packaging, wrapping or coating) plays an important role on the conservation, distribution and marketing of foodstuffs. [7] Because they are both a packaging and a food component, ideal edible films and coatings have to fulfill the following specific requirements:

- → Do not contain toxic and allergic components;
- → Provide structural stability and prevent mechanical damage during transportation, handling, and display;
- → Have good adhesion to surface of food to be protected providing uniform coverage;
- → Control water migration both in and out of protected food to maintain desired moisture content;

- → Provide semi-permeability to maintain internal equilibrium of gases involved in aerobic and anaerobic respiration, thus retarding senescence;
- → To prevent loss or uptake of components that stabilize aroma, flavor, nutritional and organoleptic characteristics necessary for consumer acceptance while not adversely altering the taste or appearance;
- → To provide biochemical and microbial surface stability while protecting against contamination, pest infection, microbe proliferation, and other types of decay;
- → To maintain or enhance aesthetics and sensory attributes (appearance, taste, etc.) of product;
- → To serve as carrier for desirable additives such as flavor, fragrance, coloring, nutrients, and vitamins. Incorporation of antioxidants and antimicrobial agents can be limited to the surface through use of edible films, thus minimizing cost and intrusive taste;
- → To be easily manufactured and economically viable. [1]

2.1.1 Biopolymers

Biopolymers are polymers generated from renewable natural sources, often biodegradable and nontoxic. They can be produced by biological systems (i.e. microorganisms, plants and animals), or chemically synthesized from biological materials (e.g., sugars, starch, natural fats or oils, etc.). Two strategies are applied in converting these raw materials into biodegradable polymers: extraction of the native polymer from a plant or animal tissue, and a chemical or biotechnological route of monomer polymerization. [8] [7]

Figure 2.1 shows a scheme representing the origin of some groups and families of biopolymers.

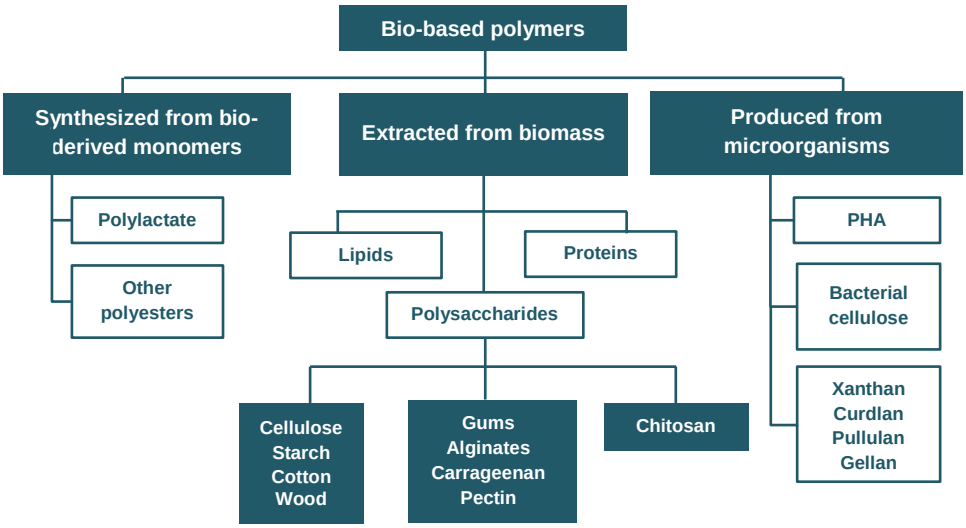

Figure 2.2 – Bio-based polymers by its origin and production method (Adapted from [9]).

Polysaccharide films, also referred to as carbohydrate-based films, are hydrophilic matrices and therefore exhibit very low moisture barrier properties. Most of the efforts for improvement were originally devoted to cellulose and starch. Such polysaccharides are of prime interest because of their availability and rather low cost, but the low elasticity of the materials is an important

drawback that limits their application. A variety of polysaccharides and their derivatives have been used as biodegradable film-forming matrixes. Beyond starch and starch derivatives and cellulose derivatives, alginate, pectin, carrageenan, chitosan, and various gums have been used as well. The major mechanism of film formation in the polysaccharide films is the breaking apart of polymer segments and reforming of the polymer chain into a film matrix or gel by evaporation of a solvent creating hydrophilic and hydrogen bonding. [2]

2.1.2 Chitosan

Chitosan, a natural biopolymer obtained from the exoskeletons of crustaceans and arthropods, is known for its unique polycationic nature and has been used as active material for its antifungal and antibacterial activity. [10].

During crustacean processing, shell wastes accounting for up to 60% of the original material are produced as a waste byproduct. One of the great problems of seafood industries is the disposal of this solid waste. These shells are rich in $CaCO_3$, protein and polysaccharide, chitin. Chitin is the second most abundant natural biopolymer after cellulose and is the major structural component of the exoskeleton of invertebrates, insects, yeast, and cell walls of fungi. By a simple demineralization (treatment with hot diluted HCl) and deproteinization (treatment with hot diluted NaOH) steps, the amino polysaccharide chitin can be quantitatively recovered from crustacean wastes. [11]

Chitosan is the N-deacetylated derivative of chitin (by treatment with hot alkali), with a structure composed of 2-amino-2-deoxy-β-D-glucose (GlcN) in a β(1,4) linkage, and with occasional N-acetyl glucosamine (GlcNAc) residues. The structure of chitin and chitosan resembles cellulose except at position C-2, being replaced by acetamido and/or amino groups, respectively (Figure 2.3). [12] [11]

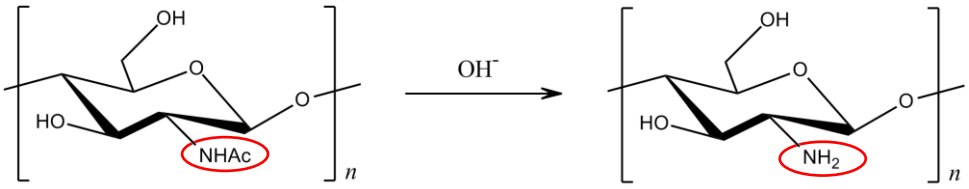

Figure 2.3 – Chemical structure of chitin and chitosan.

Because of their diversified range of application, both chitin and chitosan are biomolecules with great potential. They are essentially derived from renewable sources, biodegradable and therefore do not pollute the environment; they are biocompatible not only in animal but also in plant tissue; are nontoxic and biologically functional. Biocompatibility of chitosan allows its use in various biomedical applications. [6] [8]

The use of chitosan films and composite coatings to extend the shelf-life and improve the quality of fresh, frozen and fabricated foods was examined due to is excellent film forming properties. Chitosan films have been proposed for use in food processing, membrane separation, chemical engineering, medicine, and biotechnological areas. Due to its ability to form semipermeable films chitosan can be expected to modify the internal atmosphere as well

as decrease transpiration loss and delay the ripening of fruits. The mechanical properties, permeability, thermal decomposition points, solvent stability, etc., are parameters considered vital for selection of the right film for specific applications. [3]

Polymer blending is as effective method for providing new desirable polymeric materials for a variety of applications. Plasticizing agents are important ingredients generally used to overcome the brittleness of the biopolymeric films. Brittleness is an inherent quality attributed to the complex/branched primary structure and intermolecular forces of natural biopolymers. Plasticizers soften the rigidity of the film structure, increase the mobility of the biopolymeric chains, and reduce the intermolecular forces, thus improving the mechanical properties (elongation). [7]

With vegetables, modification of the surrounding environment can be done by individual coating of the vegetables or by sealing in the polymeric films. Chitosan films were also useful in extending the shelf-life of vegetables. Wax is extensively used as a coating material, but it enhances the risk of off-flavor development and fermentation due to drastic reduction in gas permeability of the peel. Use of plastic films for different citrus species (lemons, oranges, and grapefruits) has given better responses than waxing in preserving the overall quality, shrinkage, softening, deformation, and flavor loss. [1]

2.1.3 Additives

A number of additives can be included in the formulation of a coating solution, which will alter the properties of the resulting coating layer or freestanding film to improve performance (Table 2.1). Composite biopolymer films can bring about improved mechanical and physical properties if components are structurally compatible. Plasticizers are one of the components of edible films, they are low molecular weight compounds that are added to soften the rigid structure of films. Plasticizers improve mechanical, barrier and physical properties of biopolymers films. They must be compatible with film-forming polymers, and reduce intermolecular forces and increase mobility of polymer chains. Hydrophilic compounds such as polyols and polyethylene glycol are commonly used as plasticizers in hydrophilic film formulations. Lipophilic compounds, such as vegetable oils, lecithin and, to a less extent, fatty acids, may also act as emulsifiers and plasticizers. [1] [7]

Table 2.1- Additives used in the majority of the polysaccharide films (Adapted from [2]).

ADDITIVES	
Plasticizers	**Functional Ingredients**
Glycerol Propylene glycol Polyethylene glycol Sorbitol Water	Antimicrobials Antioxidants Flavour Colorants Vitamins Other nutraceuticals

Food additives such as antioxidants, antimicrobial agents and nutrients, can be incorporated in film formulations to achieve specific functionalities; this concept of “active films” is a very promising application as it creates new avenues for designing packaging materials. [1]

Addition of lipids to a coating solution can improve barrier properties of the resulting coating. [13]. The addition of high melting point waxes has been shown to be particularly effective in improving moisture barrier properties of films [14]. One of the most popular and oldest techniques to protect specific fruits and vegetables is the application of natural wax and lipid coatings. Coatings are intended to protect the product against dehydration, attack by fungi, and abrasion during processing and to improve product appearance. In some products, the oils appearance limits their use. [15]

2.1.4 Emulsions

Polysaccharides and proteins are good film-forming materials giving rise to excellent mechanical and structural properties, but poor moisture barrier efficiency. Therefore, hydrophobic properties of lipids are exploited for their great water barrier properties, and especially high melting point lipids such as beeswax or carnauba wax [16], [17]. To overcome their poor mechanical resistance, they can be used in association with hydrophilic material either by forming an emulsion of the lipid or by laminating the hydrocolloid film with a lipid layer [18]. Emulsion-based films are less efficient against water transfer than bilayer films because of the non-homogeneous distribution of lipids. However, they have the advantages to exhibit good mechanical resistance and to require a single step during the manufacture and application process against one step per layer for multilayer films. It has been shown for emulsion-based films that the smaller the lipid globule size is, and the more homogeneously distributed they are, the lower the water vapour permeability. [18] [19]

During emulsification, the interfacial area between the continuous and the dispersed phases is considerably augmented compared to the interface before dispersion. The interfacial free energy is therefore significantly increased. In accordance with the thermodynamic dictum that all the systems evolve towards their global energy minimum state, emulsions rapidly tend to phase separate in order to minimize the interfacial contact area and free energy. This instability manifests itself by various mechanisms: flocculation, coalescence, creaming and breaking (Figure 2.4). [20]

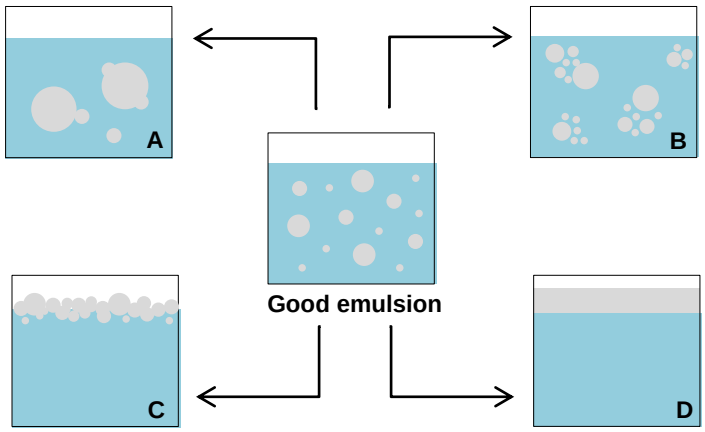

Figure 2.4 – Good emulsions and failed emulsions. (A – Coalescence; B – Flocculation; C – Creaming; D – Breaking).

Flocculation and coalescence are the major destabilization mechanisms. Flocculation and creaming are reversible mechanisms of droplets migration, whereas breaking and coalescence are non-reversible mechanisms of droplets size increase.

The nature of interactions between proteins and lipids, or between polysaccharides and lipids, determines the characteristics of emulsion formulations. In protein-lipid emulsions, proteins play a major role in stabilizing the system. Due to the amphiphilic character of proteins, they orient at the protein-lipid interface so that the non-polar groups align toward the oil and the polar groups align towards the aqueous phase. Therefore, the stabilization of the emulsion results from a balance between forces of a different nature, mainly electrostatic and hydrophobic. While protein-lipid emulsions are mainly stabilized by electrostatic forces, polysaccharides stabilize emulsions by stearic effects. To be good stabilizers, polysaccharides should be strongly attached to the surface of the lipid and also protrude significantly into the continuous phase to form a polymeric layer or a network of appreciable thickness. However, in many cases polysaccharides possess a limited amphiphilic character, so the addition of emulsifiers is required to improve emulsion stability. [19]

Issues of lipid type, location, volume fraction, and drying conditions in emulsion composite films have been studied, as affecting the barrier properties of protein and polysaccharide-based emulsion films. The results show that the moisture-barrier properties of emulsion films can be improved by using viscoelastic lipids, increasing lipid content, reducing lipid particle size, and improving film-drying conditions. [21] [18] [19] [22] [20] [16]

3 MATERIALS AND METHODS

3.1 PREPARATION OF CHITOSAN AND CHITOSAN/BEESWAX FILMS

Chitosan purchased from Golden-Shell Biochemical Co.,Ltd., China (>85% deacetilation degree) was dissolved in an acetic acid (1%wt) solution, at a concentration of 1.5%wt. After stirring overnight at ambient temperature, glycerol (50%wt, mass of glycerol per mass of dried polymer) and tween 80 (0.15%wt) were added. Then the solution was centrifuged to remove undissolved particles of chitosan and impurities. Centrifugation was performed for 30 min at a speed of 13000 rpm at a temperature of 5ºC.

For the preparation of chitosan/beeswax solutions, solid beeswax was added (1%, 5% and 10%wt, mass of wax per mass of dried polymer) to the previous solution, under stirring at controlled temperature (T=70ºC). The dispersion of the melted beeswax was promoted by vigorous magnetic stirring (1000 rpm) for 30 min. If necessary, air bubbles were removed in vacuum at room temperature.

The chitosan solutions (Ch) or the chitosan/beeswax emulsions (Ch + BW) were transferred to Teflon petri dishes and dried at 30ºC during 48 hours to form a film.

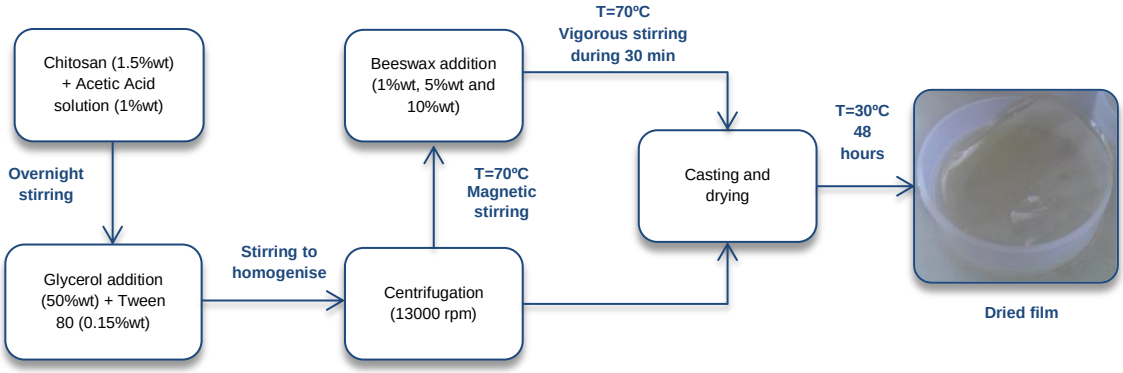

Figure 3.1 – Schematic representation of films preparation.

3.2 OPTICAL AND SUPERFICIAL PROPERTIES

3.2.1 Colour measurements

The colour alterations on objects due to the application of the films prepared was evaluated by measuring the colour parameters of coloured paper sheets, covered and uncovered by the test films. A Minolta CR-300, USA, colorimeter was used, and the CIELAB colour space was applied.

CIELAB model, relies on a model proposed by the *Commision Internationale de l'Eclairage* and which colours scale relies on the opposite colours theory. In this model, the L* defines

luminosity which range between 0 (black) and 100 (white), and the a* and the b*, are chromatic components which range between -60 and +60 and indicate, respectively, red/green value and yellow/blue value.

This model can specify colour stimulations in a tri-dimensional space, and it can be schematically represented (Figure 3.2) in a graphic whose coordinates x, y and z are relative to a*, b* and L*. As L* can be represented in the z axe, the chromatic components of the model can be represented in x and y axes, where the x represents the range between green/red, the y represents the range between yellow/blue, and the central point is the color grey.

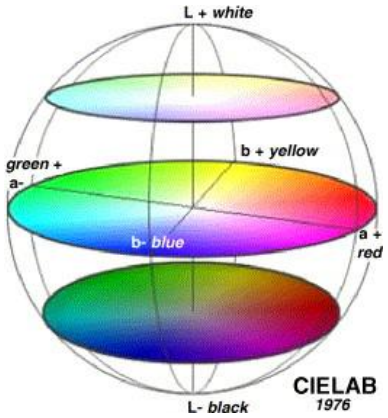

Figure 3.2 - CIELAB model representation (-a* - green; +a* - red; -b* - blue; +b*- yellow; L*(0) - black; L*(100) - white). [23]

From this model other two parameters can be obtained, C* (chroma) that is the color saturation and hº (hue) that is the color space region. The saturation is given by the Euclidian distance between chromaticity and chromatic point, and color hue is the angle between color and the origin, by the Equations 3.1 and 3.2.

$$C^* = \left(a^{*2} + b^{*2}\right)^{1/2} \quad \textbf{(Eq. 3.1)}$$

$$h^{\circ} = \tan^{-1}\left(\frac{b^*}{a^*}\right) \; when \; a^* > 0, b^* > 0$$

$$h^{\circ} = 180^{\circ} + \tan^{-1}\left(\frac{b^*}{a^*}\right) \; when \; a^* < 0 \quad \textbf{(Eq. 3.2)}$$

Color difference, ΔE, is given by the difference between L*, a* and b* of two colors (Eq. 3.3). For low values of ΔE, particularly below 10, the differences between colors are minor, but above ΔE=3 the differences are identifiable by the human eye. [24]

$$\Delta E = [(\Delta a^*)^2 + (\Delta b^*)^2 + (\Delta L^*)^2]^{1/2} \quad \textbf{(Eq. 3.3)}$$

In this work, six measurements on different areas of the colored paper sheets, with and without films, were performed.

3.2.2 Transparency

Film transparency was determined with rectangular strips of the films (9 mm x 30 mm) directly placed in a UV-Visible spectrophotometer test cell. The absorption spectrum of the sample was obtained at 600 nm in a UV-Visible spectrophotometer (*Helλos α*, *Thermo Spectronic*, UK). After transform the absorbance data in transmittance (Eq. 3.4), the transparency of the films were determined by the Equation 3.5.

$$A_{600} = -\log_{10} T_{600} \quad \textbf{(Eq. 3.4)}$$

$$Transparency = \frac{-\log_{10}(T_{600})}{\delta} \quad \textbf{(Eq. 3.5)}$$

Where:

A_{600} – Absorbance at 600 nm wave length;

T_{600} – Transmittance at 600 nm wave length;

δ – Thickness of the samples.

3.2.3 Contact angle

The surface energy or surface tension of the food product is a controlling factor in the process that involves wetting and coating of surfaces. The determination of surface tension usually involves measuring the contact angles that several standard liquids make with that surface. The surface energy of the solid surface is then related to the surface tensions of the liquids and the contact angles. [9]

The contact angle (θ) of a liquid drop on a solid surface is defined by the mechanical equilibrium of the drop under the action of three interfacial tensions: solid-vapor (γ_{SV}), solid-liquid (γ_{SL}), and liquid-vapor (γ_{LV}) (Figure 3.3).

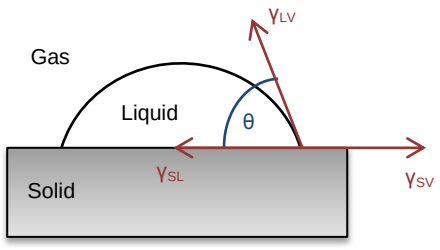

Figure 3.3 – Schematic of a sessile drop, contact angle and the three interfacial tensions are shown (Adapted from [9]).

The equilibrium spreading coefficient (W_s) id defined by Equation 3.6 and can only be negative or zero. [9] [21]

$$W_s = W_a - W_c = \gamma_{SV} - \gamma_{LV} - \gamma_{SL} \quad \textbf{(Eq. 3.6)}$$

Where W_a and W_c are the works of adhesion and cohesion, defined by Equation 3.7 and 3.8, respectively.

$$W_a = \gamma_{LV} + \gamma_{SV} - \gamma_{SL} \quad \textbf{(Eq. 3.7)}$$

$$W_c = 2 \cdot \gamma_{LV} \quad \textbf{(Eq. 3.8)}$$

The contact angle (θ) was measured by the sessile drop method. A glycerol drop is deposited manually in the film surface by a Pasteur pipette. Various photos are acquired by the software *KSV CAM 101*, which fits a mathematical function to the drop and calculates the tangent between the liquid and the film as the contact angle. The measurements were performed during 5 seconds after de drop fall.

3.3 SCANNING ELECTRON MICROSCOPY (SEM)

The analysis of the chitosan and chitosan/beeswax films was made in a scanning electron microscope Jeol JSM-7001F, *Field emission scanning electron microscope*, operated of with a beam of 10 kV. This microscope allows an observation and characterization of heterogeneous organic and inorganic materials at a nanometric (nm) and micrometric (μm) scales. It also allows tilting the sample approximately 45º, which enables the acquisition of images of the cross-section of the films beyond the images of the films surface.

The principle of this type of microscopy relies on the incidence of an electron beam in the sample surface, the type of produced signals can be secondary electron, retrodiffused, x-rays, between others. The released electrons by the beam collide with the sample surface previously treated, and in our case, secondary electrons are liberated, from which an image is obtained. The primary electron beam is mobile and scans the surface of the sample, allowing obtaining a complete image.

The sample preparation is an essential part of this essay, as the analyzed samples have to be conductors, and to achieve that, the samples are impregnated with a thin layer of gold. The treatment with gold was made in samples of film with 1 cm^2. To obtain a perfect cut, without imperfections, it was made using liquid nitrogen that allowed breaking the film without deformation of the polymer chains.

3.4 MECHANICAL PROPERTIES

Tensile and puncture tests were carried out using a TA-Xtplus texture analyzer (Stable Micro Systems, Surrey, England). All mechanical tests were performed at 22.0 ºC ± 1.0 ºC, and samples were equilibrated at 44.3% relative humidity (RH). Five replicates of each film were analyzed.

3.4.1 Tensile test

In tensile test, film stripes (25 mm x 70 mm) were attached on tensile grips A/TG and stretched at 0.5 mm/s in tension mode. The tensile stress at break (σ) was calculated as the ratio of the maximum force to the films cross-sectional area (Eq.3.9).

$$\boldsymbol{\sigma = \frac{F}{S}} \quad \textbf{(Eq. 3.9)}$$

Where σ is the tensile stress at break in Pa; F is the force to the films in N; and S is the cross-sectional area of the films in m^2.

The elongation at break (ε) was determined as the ratio of the extension of the sample upon rupture by the initial gage length (Eq. 3.10). It is an indicator to the flexibility and elasticity of the films.

$$\boldsymbol{\varepsilon = \frac{L_f - L_i}{L_i} \times 100} \quad \textbf{(Eq. 3.10)}$$

Where ε is the elongation at break, L_f is the final length in m; and L_i is the initial length in m.

This test allows the calculation of the Young Modulus (E). The Young Modulus indicates the resistance of the film to strain and can be obtained throw Eq.3.11:

$$\boldsymbol{E = \frac{\tau}{\varepsilon}} \quad \textbf{(Eq. 3.11)}$$

Where E is the Young Modulus in Pa; τ is the tensile stress in Pa; and ε is the elongation of the films. In this study, the Young Modulus was obtained by the stress/strain curves.

3.4.2 Puncture test

Puncture tests were carried out immobilizing the test film (25 mm x 25 mm) on a specially designed base with a hole of 10 mm in diameter. The samples were compressed at a speed of 0.5 mm and punctured through the hole with a cylindrical probe (2 mm diameter). The puncture stress (σ_p) was expressed as the ratio of the puncture strength by the probe contact area (Eq.3.12).

$$\sigma_p = \frac{F_p}{S_p} \quad \textbf{(Eq. 3.12)}$$

Where σ_p is the puncture stress in Pa; F_p is the force to the films in N; and S_p is the probe cross-sectional area in m^2.

This test allows the determination of strain by equation 3.13.

$$\varepsilon_p = \frac{L_f - L_i}{L_i} \times 100 \quad \textbf{(Eq. 3.13)}$$

Where ε_p is the puncture elongation; L_f is the final length in m; and L_i is the initial length in m. The parameter L_f refers to the film elongation and it's calculated with base in the elongation measured by de probe, d (Eq. 3.14). In figure 3.4 a illustrative scheme is shown.

$$L_f^{\,2} = d^2 + L_i^{\,2} \Leftrightarrow L_f = \sqrt{d^2 + L_i^{\,2}} \quad \textbf{(Eq. 3.14)}$$

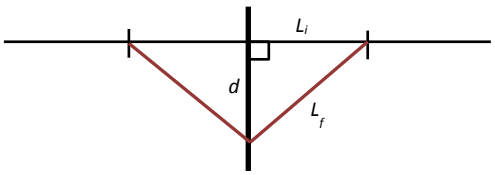

Figure 3.4 – Puncture test scheme.

3.5 WATER SORPTION ISOTHERMS

Water sorption isotherms were determined by a gravimetric method at 30ºC. Samples with dimensions of 20 mm x 20 mm were previously dried at 70ºC during 24 hours. The samples were then placed in desiccators with different saturated salt solutions: LiCl, CH_3COOK, $MgCl_2.6H_2O$, K_2CO_3, $Mg(NO_3)_2$, $NaNO_2$, $NaNO_3$, $(NH_4)_2SO_4$ and $BaCl_2$, with a water activity at 30ºC of 0.115, 0.225, 0.324, 0.447, 0.520, 0.649, 0.731, 0.806 and 0.920, respectively. The samples were weighed after 3 weeks, ensuring that the equilibrium has been reached. [25]

Using the experimental sorption data, the water sorption isotherms were assembled. [25] [14] The following models were used:

- → GAB (mathematical model based on the existence of multilayer and condensed film);
- → Halsey and C&I (semi-empirical models);
- → Oswin, Kuhn and Smith (theoretical models);

The equations corresponding to each model are presented below [14]. The parameters of the equations were obtained through the software *Origin*.

$$\boldsymbol{GAB}: \boldsymbol{m_c} = \frac{\boldsymbol{C \cdot k \cdot m_m \cdot a_w}}{(\boldsymbol{1 - k \cdot a_w}) \cdot (\boldsymbol{1 - k \cdot a_w + C \cdot a_w})} \quad \textbf{(Eq. 3.15)}$$

$$\boldsymbol{Halsey}: \boldsymbol{m_c} = \boldsymbol{C} \cdot [-\ln(\boldsymbol{a_w})]^{\boldsymbol{k}} \quad \textbf{(Eq. 3.16)}$$

$$\boldsymbol{C\&I}: \boldsymbol{m_c} = \boldsymbol{k} \cdot \left(\frac{\boldsymbol{a_w}}{\boldsymbol{1 - a_w}}\right) + \boldsymbol{C} \quad \textbf{(Eq. 3.17)}$$

$$\boldsymbol{Oswin}: \boldsymbol{m_c} = \boldsymbol{C} \cdot \left(\frac{\boldsymbol{a_w}}{\boldsymbol{1 - a_w}}\right)^{\boldsymbol{k}} \quad \textbf{(Eq. 3.18)}$$

$$\boldsymbol{Kuhn}: \boldsymbol{m_c} = \frac{\boldsymbol{k}}{\ln(\boldsymbol{a_w^{-1}})} + \boldsymbol{C} \quad \textbf{(Eq. 3.19)}$$

$$\boldsymbol{Smith}: \boldsymbol{m_c} = \boldsymbol{k} \cdot \ln(\boldsymbol{1 - a_w}) + \boldsymbol{C} \quad \textbf{(Eq. 3.20)}$$

In which m_c represents the mass of water per mass of dried solids in the equilibrium; m_m represents de value of the humidity monolayer; a_w represents the water activity; K represents a correction constant which considers the multilayer properties in the liquid film; and C represents Guggenheim constant and corresponds to the difference of energy between water molecules linked to the first layer of adsorption and the ones linked to the next layers.

3.6 WATER VAPOR PERMEABILITY

The water vapor permeability was measured gravimetrically at 30ºC. The films were sealed with silicone to the top of a glass petri dish with a 5 cm diameter as shown in Figure 3.5. The driving force tested was imposed using a saturated $(NH_4)_2SO_4$ solution $(a_w = 0.806)$ inside the petri dish and a saturated $MgCl_2.6H_2O$ solution outside $(a_w = 0.324)$. The films tested were previously equilibrated at 80.6% RH. A fan was used to promote the air circulation inside the desiccator, in order to minimize the mass transfer resistance of the air boundary layer above the membrane. [25] [27].

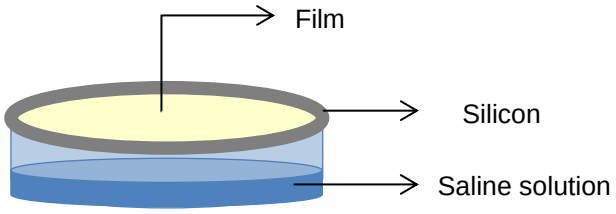

Figure 3.5 – Schematic representation of the film disposal during WVP essay.

In Figure 3.6 the WVP essay scheme is shown. The room temperature and relative humidity outsider the petri dish were measured over time using a thermohygrometer (Vaisala, Finland). The water vapor flux was determined by weighing the petri dish in regular time intervals for 8 hours. [25]

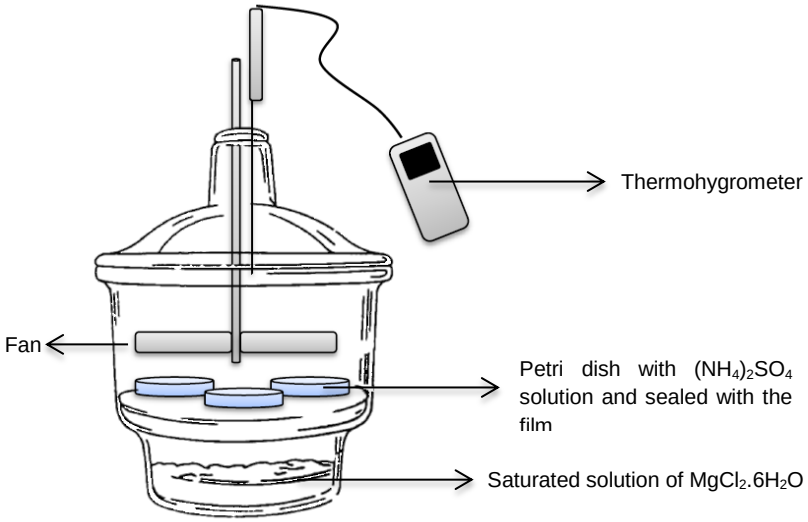

Figure 3.6 – Experimental scheme for WVP essay.

The water transport in the experimental set-up used accounts for the following steps (Figure 3.7):

i) Evaporation at the solution interface inside the petri dish,
ii) Diffusion through the stagnant film of air below the test film,
iii) Evaporation at the solution interface inside the petri dish,
iv) Water diffusion through the test film and
v) Water desorption at the film's interface outside the petri dish.

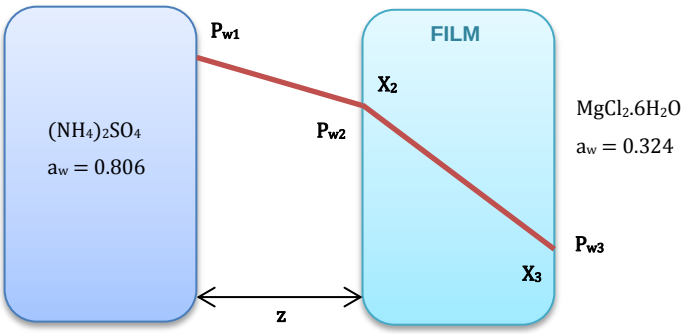

Figure 3.7 – Water vapor pressure profiles on the films boundary layers and water concentration inside the films for 80.6 – 32.4 %RH. (Adapted from [25])

The resistance to water transfer in the boundary layer above the film was neglected, since a fan was used to promote favorable hydrodynamic conditions inside the desiccator. The water vapor permeability (WVP) was calculated using Eq. 3.21.

$$\boldsymbol{WVP = \frac{N_w \times \delta}{\Delta P_{w,eff}}} \quad \textbf{(Eq. 3.21)}$$

In which, N_w is the water vapor molar flux, δ is the film thickness and $\Delta P_{w,eff}$ is the effective driving force, expressed as the water vapor pressure difference between both sides of the film, calculated taking into account the mass transfer resistance of the stagnant film of air below the test film, and is given by Eq. 3.22:

$$\boldsymbol{\Delta P_{w,eff} = P_{w2} - P_{w3}} \quad \textbf{(Eq. 3.22)}$$

The unknown value of P_{w2} was determined using Eq. 3.23, taking into account that, at steady state conditions, the measured water flux (N_w) is equal to the flux through the stagnant film of air that separates the surface of the liquid from the surface of the test film:

$$\boldsymbol{N_w = \frac{P}{RTz} D_{w-air} \ln\left(\frac{P - P_{w2}}{P - P_{w1}}\right)} \quad \textbf{(Eq. 3.23)}$$

Where P is the atmospheric pressure, R the gas constant, T the temperature, z the distance from the test film to the solution's surface, D_{w-air} is the water vapor diffusion coefficient in air, P_{wi} is the water partial pressure contacting the liquid surface and the test film (Eq. 3.24).

$$\boldsymbol{P_{wi} = a_{wi} \times P_w^*} \quad \textbf{(Eq. 3.24)}$$

The value of P_{w1} is known, and was calculated with the water activity of the liquid phase (a_{w1}) and the water vapor pressure (P_w^*). The water partial pressure outside the petri dish (P_{w3}) was calculated using the measured %RH values (Eq. 3.25).

$$\boldsymbol{P_{w3} = a_w P_w^* = \frac{\%RH \times P_w^*}{100}} \quad \textbf{(Eq. 3.25)}$$

The molar water flux (N_w) through the test film at steady-state may be expressed using Eq. 3.26, which is based on the first Fick's Law:

$$\boldsymbol{N_w = \frac{D_{eff} \rho_s}{M_w} \frac{X_2 - X_3}{\delta}} \quad \textbf{(Eq. 3.26)}$$

In which ρ_s is the dry film density, M_w is the water molar mass, X_i is the water concentration (mass of water/mass of dry polymer) in both film interfaces ($X_2 > X_3$) and δ is the film thickness

(Figure 3.7). At equilibrium, the X_i values may be related to the water activity using the water sorption isotherms by Eq.3.27.

$$S_i^* = \tan(\theta) = \frac{X_i}{a_{wi}} \quad \textbf{(Eq. 3.27)}$$

Where $S_i^*[g_{water}/g_{solids}]$ the water sorption coefficient of the film material, which is can be converted to $S_i[g_{water}/g_{solids}Pa]$ by dividing Eq.3.27 by the pure water vapor pressure:

$$S_i = \frac{X_i}{a_{wi}P_w^*} \quad \textbf{(Eq. 3.28)}$$

Combining Eq.3.26 e 3.28, an expression which enables the determination of the effective diffusion coefficient is obtained (Eq.3.29) [25]:

$$D_{eff} = \frac{N_w M_w}{\rho_s P_w^* (S_2 a_{w2} - S_3 a_{w3})} \quad \textbf{(Eq. 3.29)}$$

3.7 GAS PERMEABILITY

For this essay the samples used were cut with 7 cm diameter and their thickness was measured by a manual micrometer (*Braive Instruments*, USA).
The experimental apparatus used is composed of a stainless steel cell with two identical chambers separated by the test film. The films were previously equilibrated at a constant relative humidity of 52.0 %RH. The permeability was evaluated by pressurizing one of the chambers (feed) up to 700 mbar, with pure carbon dioxide or oxygen followed by the measurement of the pressure change in both chambers over time, using two pressure transducers. The measurements were made at a constant temperature, 30ºC, using a thermostatic bath (*Julabo*, Model EH, Germany) (Figure 3.8).

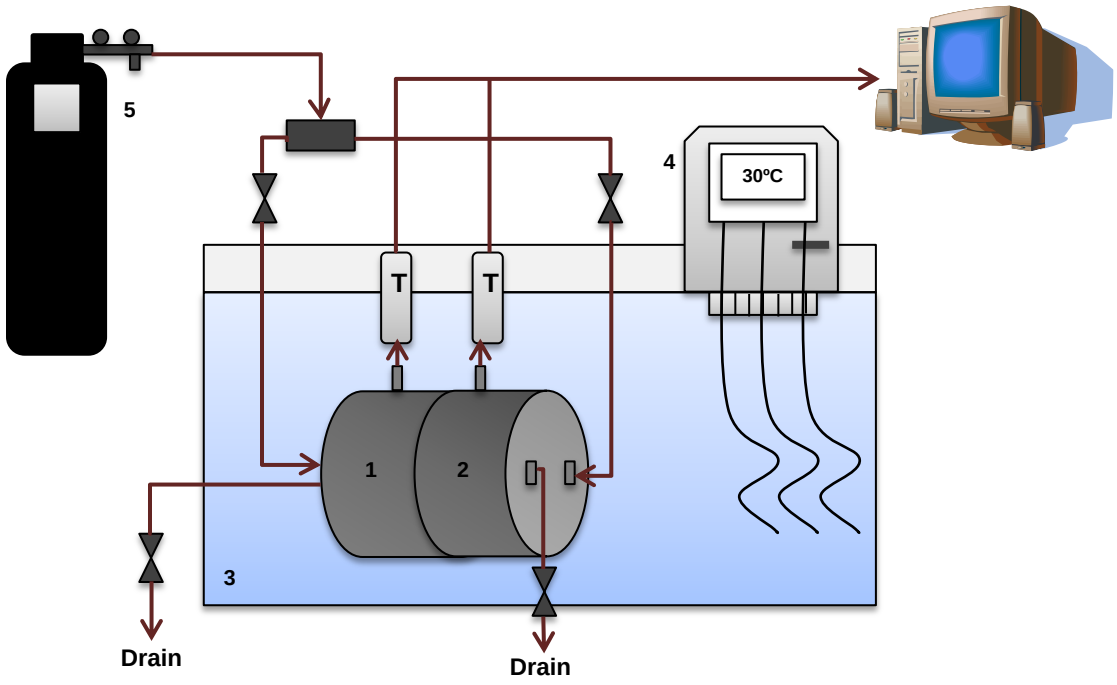

Figure 3.8 – Experimental gas permeation setup (1 – Feed; 2 – Permeate; 3 – Water bath; 4 – Bath head, 5 – Feed gas).

The permeability was calculated with the pressure data obtained from both compartments and by the software *Origin*, according to the following equation:

$$\frac{1}{\beta}\ln\left(\frac{[p_f - p_p]_0}{[p_f - p_p]}\right) = \frac{1}{\beta}\ln\left(\frac{\Delta p_0}{\Delta p}\right) = P\frac{t}{\delta} \qquad \textbf{(Eq. 3.30)}$$

Where p_f and p_p are the pressures in the feed and permeate compartments, respectively; P is the gas permeability; t is the time; and δ is the film thickness. The geometric parameter β is $A(1/V_f + 1/V_p)$, where V_f and V_p are the volumes of the feed and the permeate compartments, respectively, and A is the membrane area. This parameter was calculated ($\beta = 160.827\ m^{-1}$) with a PDMS membrane and nitrogen as test gas, using the permeability value referred in the literature, $P_{N2/PDMS} = 2.3 \times 10^{-10}\ m^2/s$ [28]. The film sample gas permeability is equal to the slope obtained representing $\ln(\Delta p_0/\Delta p)$ as a function of $\beta t/\delta$ (ANNEX I). [25]

4 RESULTS AND DISCUSSION

4.1 CHITOSAN AND CHITOSAN/BEESWAX FILMS

Homogeneous and flexible films were obtained after drying at 30ºC. Visually, all films were transparent with a slightly yellowish coloration as found out by naked eye observation. The films thickness is $60 \pm 10\ \mu m$.

Figure 4.1 – Chitosan films.

The obtained chitosan films are shown in Figure 4.1, and the chitosan-beeswax films in Figure 4.2. As we can see the chitosan films are all homogeneous and transparent.

Figure 4.2 – Chitosan-beeswax films. A – 1% BW; B – 5% BW; C – 10% BW.

It is not possible to notice in the photographs presented on Figure 4.2, but the yellowish coloration of the films slightly increase as the amount of incorporated besswax increases. Regarding to the homogeneity, the films Ch + 10%BW have some imperfections, small clusters of wax, due to less efective emulsion forming process. All this characteristics can be observed by naked eye.

4.2 OPTICAL AND SUPERFICIAL PROPERTIES

Optical and superficial properties are essential to define the ability of films and coatings to be applied over a food surface, since these affect the appearance of the coated product, which is an important quality factor. [29]

One important aspect in appearance is haze, a term that refers to the tendency of light-transmitting plastics to scatter light, producing a cloudy appearance as a result. The effect of haze is largely aesthetic, although in extreme cases haziness may interfere with one's ability to distinguish details of contents in packages that are important to consumers. Biopolymer coatings have the potential to improve the visual quality of foods, especially appearance, because of their high gloss and transparency. [30]

4.2.1 Colour measurements

The L*a*b* colour model allows the study of the differences introduced by the films in the coloured cardboards. In **Erro! A origem da referência não foi encontrada.** there are represented the ΔE values for the Ch and Ch + BW films prepared, these values show the differences between the coloured cardboards with or without the films.

Table 4.1 - ΔE values (colour differences between the cardboards with or without film).

Film	White	Blue	Yellow	Green	Red
Ch	9	13	9	9	11
Ch + 1% BW	12	15	7	8	9
Ch + 5% BW	16	16	7	7	8
Ch + 10% BW	12	15	7	8	9

Since ΔE > 3, it can be concluded that the superposition of the films with the coloured cardboards induces an alteration that can be identified by the human eye. For all the colours ΔE values are very close to 10 and for the white and blue colours the alterations are more significant, so the introduction of the films promotes colour alteration on the surfaces, especially for white and blue surfaces.

For a better interpretation of the results, Figure 4.3 shows a graphic representation of the experimental results, in Figure 4.3.B the colour plan a*b* and in Figure 4.3.A a 3D representation of the colour plan L*a*b*.

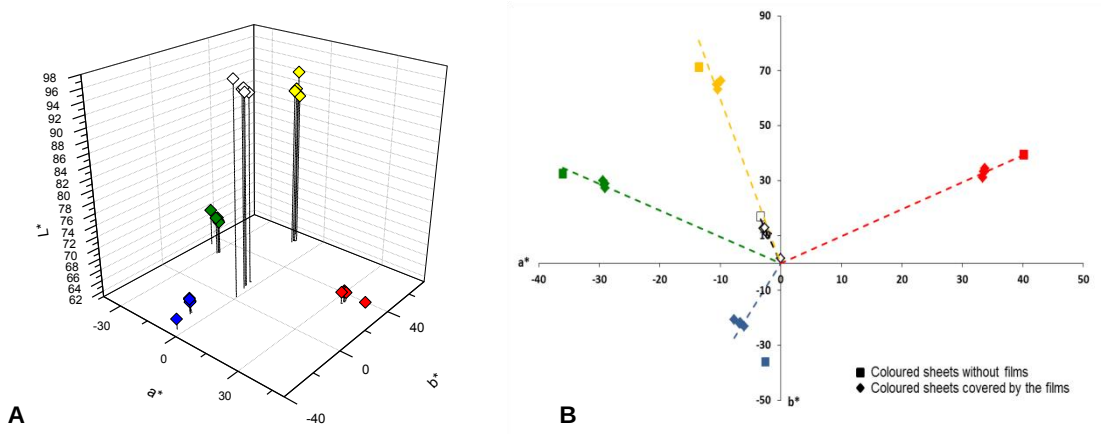

Figure 4.3 – Graphic representation of the films colour according to SCIELAB model (A - 3D representation of the coordinates L*a*b*; B – representation of the a*b* plan).

Analysing the a*b* plan representation, it can be clearly seen that the points corresponding to the coloured cardboards without film and the ones corresponding to the films superposition are very near for each colour represented. The 3D representation provides a better perception of the spatial distribution of the colours and once more confirms that there are no significant alterations in the cardboards colour with or without films since the points in the graphic are distributed in the same region and very close to each other for the same colour.

In **Erro! A origem da referência não foi encontrada.** the colour saturation (C*) values for the cardboards and the cardboards with the films are shown. A slightly decrease in the colour saturation can be observed for the samples with film as the content in beeswax increase for all colours except for the colour white where it can be noticed an increase in colour saturation for the samples with film. It can be stated that the colour became a little less intense, as it can be confirmed by the approximation of the points to the graphic origin in a*b* plan.

Table 4.2 - Representation of the films color saturation (C*).

Sample	White	Blue	Yellow	Green	Red
No film	1.73	36.06	72.61	48.53	56.25
Ch	10.87	23.76	64.00	39.80	45.62
Ch + 1% BW	13.00	22.92	65.75	40.77	47.24
Ch + 5% BW	17.27	22.02	67.13	41.95	48.19
Ch + 10% BW	13.19	22.71	66.26	40.87	47.14

Table 4.3 - Representation of the films colour hue (hº).

Sample	White	Blue	Yellow	Green	Red
No film	91.08	265.94	100.73	137.94	44.46
Ch	101.88	255.32	99.39	136.88	43.02
Ch + 1% BW	103.05	252.62	99.31	135.69	44.78
Ch + 5% BW	101.14	249.58	98.45	134.48	45.59
Ch + 10% BW	101.14	253.05	98.93	135.21	44.51

The angle hº, that represents the hue of the colour stays practically constant for each colour, suffering only slight alterations, except for the blue and the white, as it can be seen in Table 4.3.

4.2.2 Transparency

The transparency parameter was calculated by determining the ratio of the transmittance logarithm coefficient at 600 nm by the films thickness. For a better evaluation of the obtained results, Figure 4.4 presents a graphic where it can be seen the relation between the transparency and the amount of beeswax in each film. The films thickness shows a very high standard deviation because several samples of several different films were used (scraps from films used in other experiments).

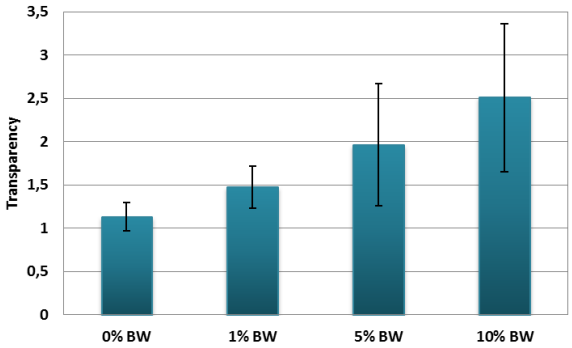

Figure 4.4 – Graphic representation of the transparency of the films.

It can be seen an increase in the transparency parameter values as the amount of incorporated beeswax increases. This means that the films barrier properties to light become higher. The beeswax addition beyond introducing a yellowish colour in the films increases (not very significantly) the films opacity.

4.2.3 Contact angle

Surface properties of the films (i.e., contact angle) give information about the phenomenon of wetting or non-wetting of a product surface by film forming dispersions and thus, about the uniformity of coating when applied to a particular solid surface. Moreover, the contact angle method is a simple way to determine the superficial hydrophilicity of films since when using water or another polar solvent, contact angle will increase with increasing surface hydrophobicity. [29] [31]

For these reasons, the contact angle of the films was measured using glycerol as the polar solvent. The essay results are represented in Figure 4.5. It can be observed a decrease of the contact angle over the time, what reflects the hydrophilic character of the films surface, more pronounced for the films without beeswax incorporation.

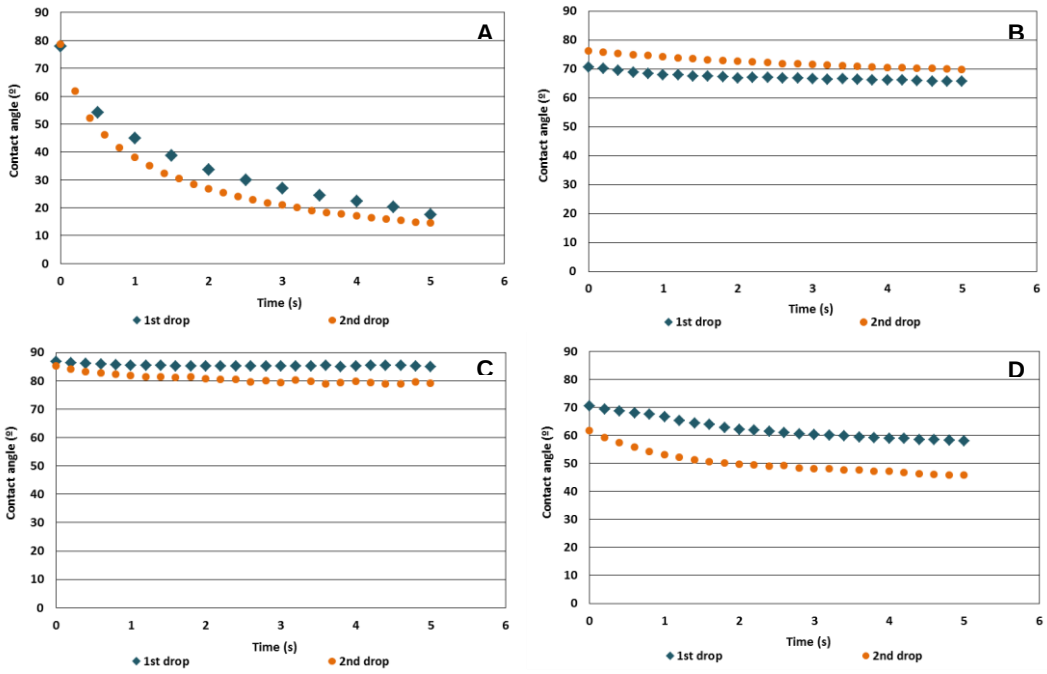

Figure 4.5 – Variation of the contact angle over time (A – Ch films; B – Ch + 1% BW films; C – Ch + 5% BW films; D – Ch + 10% BW films).

It is important to refer that in this type of essay, the associated error is very high, since the operator has a direct contact whit the experience and that influences all the process. In each essay several film samples and several drops were used. To obtain the average values the samples chosen were the ones that presented the best drop (more perfect) and the nearest contact angle values. Each essay held for 5 seconds in order to obtain coherent results. In figure 4.6 the contact angle variation with the beeswax content of the films is shown.

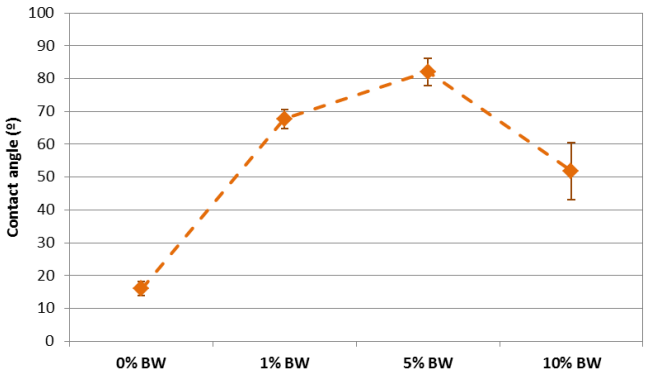

Figure 4.6 – Evolution of the contact angle of the films with the increase in the beeswax content.

As expected, the contact angle is lower for the chitosan films without beeswax addition. These films are extremely hydrophilic, so that when a drop of water was placed in its surface (instead

of glycerol) an instantaneous absorption occurred that ended up deforming the film. For the films with incorporation of beeswax the contact angle increases comparing with the Ch films, due to the increase in the surface hydrophobicity. For the Ch + 10% BW films there is a decrease in the contact angle in relation to the films with 1% and 5% beeswax. This behavior is due to a lack of uniformity in the dispersion. In these films with higher content in beeswax it can be observed by naked eye some beeswax agglomerate areas, which causes the polar solvent a tendency to seek the most hydrophilic region of the film, thereby escaping these hydrophobic areas. During the essays it was observed that the drops of glycerol deposited on the films with 10% BW end up deforming as they spread through the film. In contrast with the other films which present a uniform spreading.

Generally, it can be said that the incorporation of beeswax in the chitosan films increases its hydrophobic character due to the presence of the dispersed lipids in the chitosan hydrophilic matrix. [31] [29]

4.3 SCANNING ELECTRON MICROSCOPY (SEM)

For an interpretation of the structure and properties of the films, a SEM analysis of the surface and cross-section of the films was performed. In Figure 4.7 the surface images of the films obtained for $4000\times$ magnification are shown.

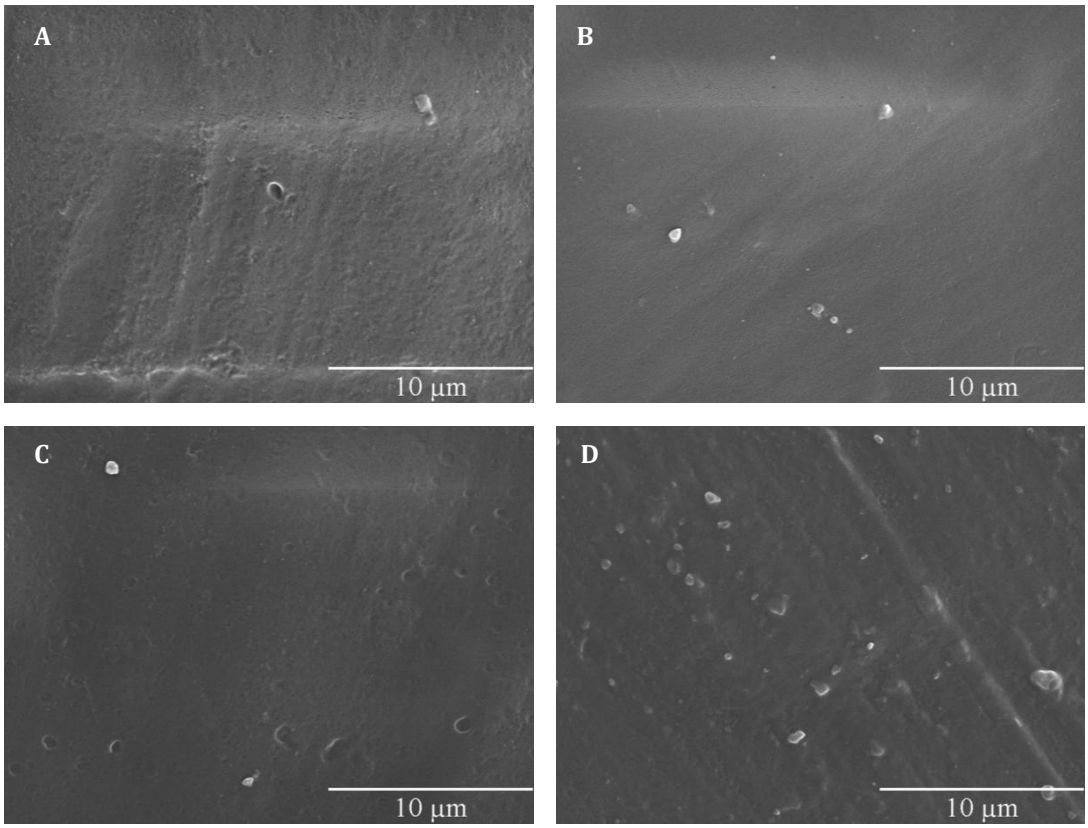

Figure 4.7 – Surface of the films with a magnification of 4000 x (A – Ch films; B – Ch + 1% BW films; C – Ch + 5% BW films; D – Ch + 10% BW films).

It was observed that all the films present a dense structure; the light particles observed are probably dust (they are not incorporated in the film matrix but at its surface). The dark areas in the films with beeswax incorporation are little depressions, probably fused beeswax particles incorporated in the films structure.

In Figure 4.8 images of the cross-section of the films for $600\times$ magnification are shown. The cut of the films was made using liquid nitrogen in order to preserve the structure of the films. All the films show a dense and homogeneous structure whereas when there is addition of beeswax small irregularities in the films are noted. However there are not pores or cracks in its structure.

In order to better understand the alterations imposed by the incorporation of different percentages of beeswax, in Figure 4.9 are represented the images of the cross-section of the films with beeswax incorporation with $4000\times$ magnification.

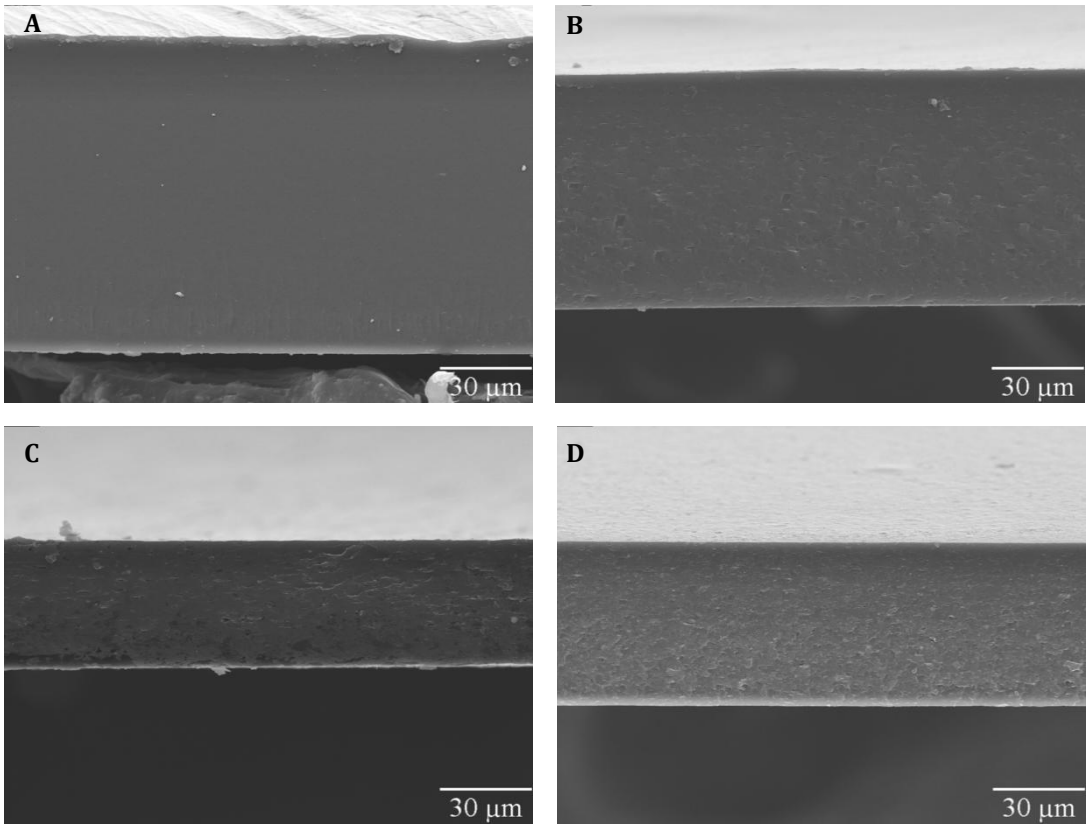

Figure 4.8 – Images of the cross-section of the films with a magnification of 600 x (A – Ch films; B – Ch + 1% BW; C – Ch + 5% BW; D – Ch + 10% BW).

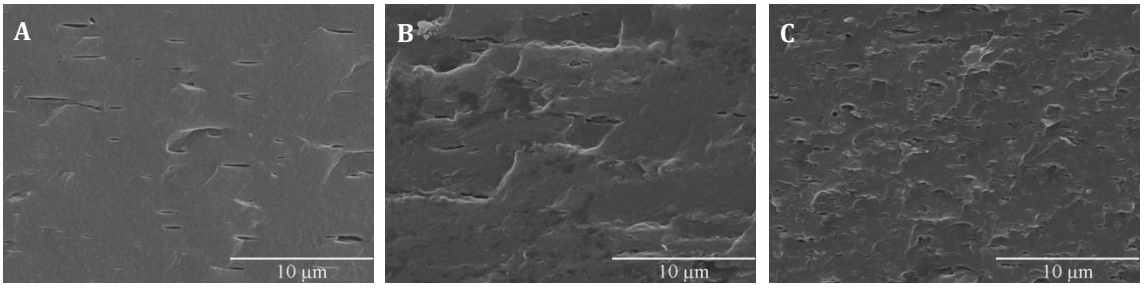

Figure 4.9 – Images of the cross-section of the films with a magnification of 4000 x (A – Ch + 1% BW film; B – Ch + 5% BW film; C – Ch + 10% BW film).

The samples prepared with beeswax show structural discontinuities according to the immiscibility of the components of the film. These irregularities increase with increasing beeswax content of the films. The irregular form of the particles in the films prepared with beeswax reveals the solid state of these particles during the formation of the films. Solvent evaporation during the drying process of the filmogenic emulsion induces changes in the emulsion structure due to phenomenon of destabilization like flocculation and coalescence of droplets. The intensity of this phenomenon depends on the concentration of lipid, the particles size in the initial emulsion, the viscosity of the continuous phase and the properties of the interfacial surface of the droplets. [29] [22]

The lower the melting point of the lipid, the easier the emulsion is and the smaller the size of the droplets. The droplet formation and its development during the drying of the film suppose the discontinuation of the polymeric matrix, increasing the intern heterogeneity and the irregularity of the film surface. [32].

These irregularities are more pronounced with increase of the percentage of beeswax incorporated, in accordance with the highest ratio of non-polar lipids.

4.4 MECHANICAL PROPERTIES

The suitable use of edible packaging strongly depends on their favourable barrier and mechanical properties. The loss of mechanical integrity in edible films and coatings due to poor mechanical properties reduces their effectiveness as a barrier. The study of mechanical properties of edible films is a subject of great importance due to their influence on the product and consumer acceptance. [33]

4.4.1 Tensile test

Figure 4.10 shows representative stress-strain curves obtained from tensile tests, for all the films under study. It can be observed that the deformation at room temperature, under an applied load, was typical of ductile plastics in terms of the stress and strain. [33]

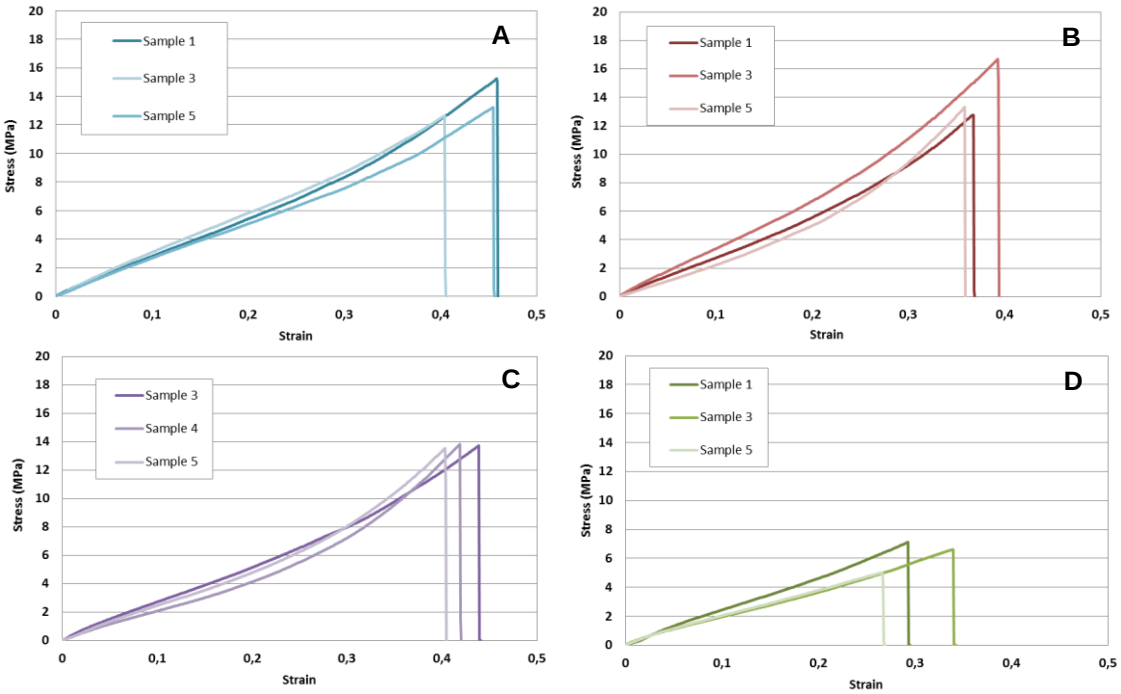

Figure 4.10 – Stress-strain curves from the tensile test. A – Ch films; B – Ch + 1%BW films; C – Ch + 5%BW films; D – Ch + 10%BW films.

At low strains the stress increased more slowly with an increase in the strain and the slopes were in the elastic region defining the elastic modulus or Young's modulus. At higher strains the stress increased rapidly until failure occurred.

In Figure 4.11 a graphic of the mechanical properties is presented. It can be seen that the incorporation of beeswax into the chitosan matrix tends to decrease the Young modulus and stress at the break, turning the matrix less resistant to the deformation. In addition, the strain at break also decreases, which may be attributed to the phase discontinuities introduced by the beeswax throughout the chitosan layer. These effects are more visible for the films with the highest wax content.

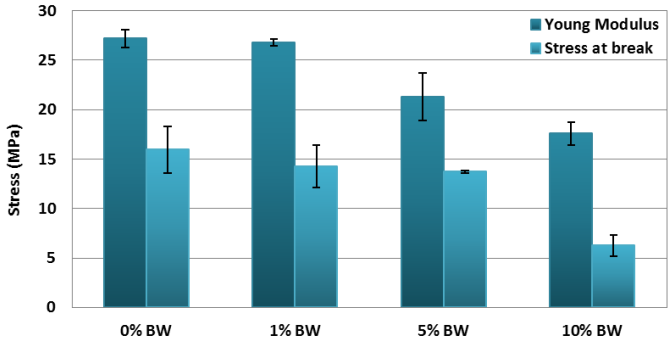

Figure 4.11 – Young modulus and stress at break in the tensile test.

The incorporation of lipids in a polymeric matrix can cause a disruption in this matrix continuity inducing the development of a heterogeneous film structure, decreases the water affinity which reduces the water plasticizer effect on the film mechanical properties. All this factors resulted in a decreased Young modulus [34] [35]. These discontinuities will affect the elongation of the films, depending on the lipid characteristics, for example the physical state. During the stretch of the film, the droplets of lipid can be easily deformed as liquids but this doesn't happen when they are solid, on the contrary, the solid droplets form a rigid disperse phase in the films what reduces its capacity of elongation [22], as it is observed in the present work.

It is difficult to make an effective comparison with the results obtained from other authors since there is a great dispersion in the literature associated with the different chitosan compositions, film preparation methods and conditioning before the tests.

Table 4.4 - Mechanical properties from the tensile test comparison.

Film	Plasticizer	Young Modulus (MPa)	Stress at break (MPa)	Elongation at break (%)	Reference
EPS	-	1738.5	51	9.5	[27]
k-carrageenan	-	1110	57	6.8	[27]
WPI	-	84.0	3.3	27.6	[4]
Chitosan	-	11.0	23.0	22.0	[4]
Chitosan	Glycerol(1:0.28)	76.2	8.41	19.55	[29]
Ch	Glycerol(1:0.5)	27.2	15.95	48.9	Present work
Ch + 10% BW	Glycerol(1:0.5)	17.6	6.25	29.9	Present work
NaCas	Glycerol(1:0.3)	850	14.4	4.0	[22]
NaCas+25%BW	Glycerol(1:0.3)	193	2.8	3.5	[22]
WPC	Glycerol (3:1)	156	3.32	4.36	[35]
WPC+20%BW	Glycerol (3:1)	155	2.13	2.39	[35]
PP	-	798	47	933	[27]
HDPE	-	631	38	531	[27]

Making a Young modulus comparison between the films presented in Table 4.4 it can be seen that the Ch films prepared in this work present a low stiffness, as their Young modulus are quite low.

4.4.2 Puncture test

In Figure 4.12 it can be observed the stress-strain curves for the puncture test. As it can be observed by the curves behaviour the probe progressed less until the perforation of the films that in the tensile test for the breaking, so this essay is quicker than the previous one and the strain achieved is smaller.

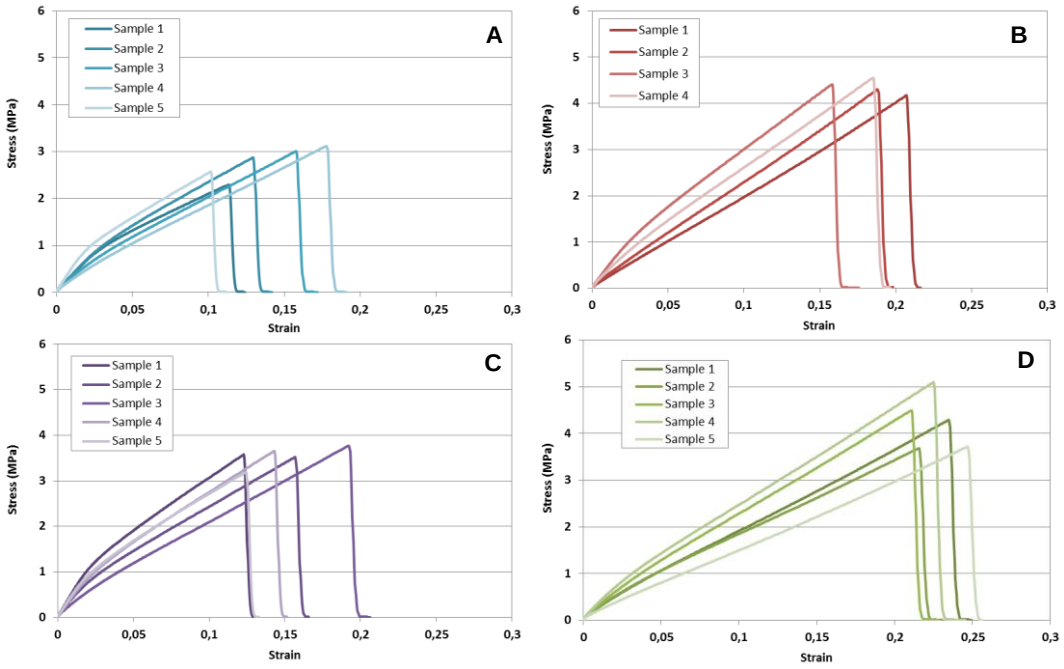

Figure 4.12 – Puncture test stress-strain curves. A – Ch films; B – Ch + 1%BW films; C – Ch + 5%BW films; D – Ch + 10%BW films.

In **Erro! A origem da referência não foi encontrada.** are presented the thickness, stress at break and elongation at break values for each studied film. For this test the films were chosen with near thickness values as this parameter influences the puncture tests greatly. [23]

Table 4.5 - Mechanical properties obtained by puncture tests and thickness of the films.

Film	Thickness (µm)	Stress at break (Pa)	Elongation at break
Ch	59.80 ± 1.09	2.76 ± 0.34	0.14 ± 0.03
Ch + 1% BW	58.50 ± 1.73	4.36 ± 0.34	0.19 ± 0.02
Ch + 5% BW	57.92 ± 1.82	3.54 ± 0.22	0.15 ± 0.03
Ch + 10% BW	59.84 ± 2.03	4.25 ± 0.59	0.23 ± 0.02

Although there is no direct relation between the amount of wax incorporated in the films and the mechanical properties calculated in this assay, it can be stated that the addition of wax increases both the tension and deformation of rupture of the films of chitosan.

Table 4.6 - Mechanical properties for the puncture test comparison.

Film	Plasticizer	Stress at break (Pa)	Elongation at break (%)	Reference
WPC	Glycerol (3:1)	2.067	8.2	[35]
WPC + 20% BW	Glycerol (3:1)	0.243	0.67	[35]
Ch	Glycerol (1:0.5)	2.76	14	Present work
Ch + 10% BW	Glycerol (1:0.5)	4.25	23	Present work

For the comparison with the literature it was difficult to find a result respecting this particular essay as the tensile test is much more used to determine the mechanical properties. Comparing the Ch films with the results of WPC (whey protein concentrate) found in the literature, it can be seen that the stress at break for both films are very similar and only in the elongation the Ch films showed more flexibility that the WPC ones. The Ch+10%BW films can be compared with the WPC+20%BW films presented in Table 4.6, for the chitosan films the beeswax incorporation increased the stress at break and the elongation at break of the films but on the contrary for the WPC films the beeswax incorporation decreased both parameters. In summary the chitosan films are always more resistant and flexible to puncture than the WPC films and with respect to the beeswax incorporation, it improved the chitosan films but weakened the WPC ones.

4.5 WATER SORPTION ISOTHERMS

Sensibility to water is a very important parameter in the evaluation of food packaging characteristics. Therefore, the study of the water vapour adsorption capacity through water sorption isotherms - that express the equilibrium relation between atmosphere water content and the film water content - is very useful. The studied chitosan films are very hydrophilic and therefore very sensitive to water, so it's extremely important to study their behaviour regarding water adsorption.

The films water sorption isotherms were adjusted with the different theoretical models presented. To make an adjustment of a non-linear curve, an iterative procedure that minimizes the reduced chi-square (χ^2) value is employed to obtain optimum values for the parameters. The reduced chi-square is obtained dividing the residual sum of squares (RSS) for the degrees of freedom (DOF). Despite this quantity being minimized during the iteration process, it is typically a bad measure to determine the adjust quality.

A better measure is the value of R^2, which is also known as determination coefficient. The nearest the adjust is to the experimental data, the nearest the R^2 value will be to 1. A higher R^2 value is not necessary a better adjust due to the degrees of freedom that can affect the value too. If more parameters are introduced the R^2 value will increase but that does not imply a better adjust. The adjusted R^2 counts to the degrees of freedom and this could be a better measure of the adjust quality. The programme Origin reports the adjusted R^2 values and the reduced chi-square for non-linear adjusts. [22]

The obtained curves are sigmoid in shape and the model that best describes the water adsorption by the films is the GAB (Guggenheim, Anderson and De Boer) model (Eq. 3.15). Other adjusted models are shown in the annexes. In **Erro! A origem da referência não foi encontrada.** the parameters values from the GAB model adjusted are presented and in Figure 4.13 the isotherms are shown.

Table 4.7 - GAB model parameters adjusted with the software Origin.

Film	m_m	C	k	$R^2_{ajusted}$	$X^2_{reduced}$
Ch	0.0512 ± 0.0079	3.9224 ± 2.5631	0.9541 ± 0.0090	0.9911	5.94×10^{-4}
Ch + 1% BW	0.0616 ± 0.0091	3.2612 ± 2.5335	0.9325 ± 0.0111	0.9891	4.37×10^{-4}
Ch + 5% BW	0.0993 ± 0.0224	1.3827 ± 0.7019	0.8640 ± 0.0227	0.9940	1.60×10^{-4}

Ch + 10% BW	0.1414 ± 0.0251	0.6751 ± 0.1651	0.8362 ± 0.0165	0.9993	2.17×10^{-5}

The curves show an increase (not constant) of the capacity of water adsorption by the films with the increase of water activity. For low water activities (multilayer adsorption region) the amount of absorbed water increases slowly and almost in a linear way, and for high water activities (capillary condensation region) the water adsorption is faster and reveals an asymptotic tendency to water activity values near 1.

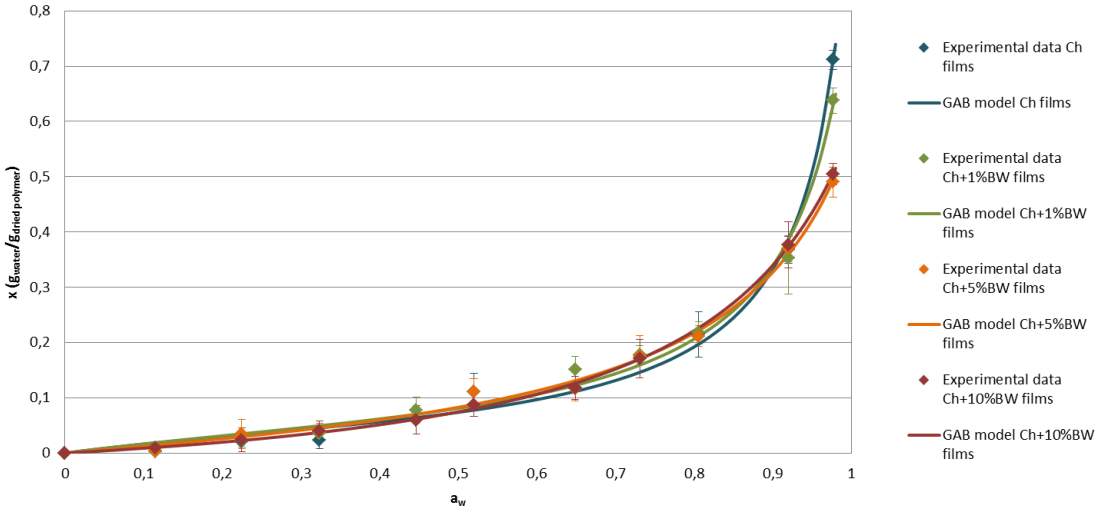

Figure 4.13 – Sorption isotherms for the chitosan and chitosan with beeswax films by the GAB model.

The same sorption isotherms behaviour in hydrophilic polymers was observed in other studies, for starch [21], EPS [23] and chitosan blends [38]. The shown behaviour is characteristic of materials constituted largely by polysaccharides [39]. Chitosan has three predominant adsorption sites: hydroxylpropyl group, amine group and polymer chain end (made up of a hydroxyl group or an aldehyde group). [31]

For low water activities the water physical adhesion in active sites of the polymer occurs only in the surface, binding to the polysaccharide hydroxyl groups. Moreover, for low water activities, there is a local dissolution of the hydroxyl groups that causes the polymer swelling and the appearance of new active sites. [21] [38] [23]

For intermediate water activities the adsorption occurs in less active regions, experiencing a gradual plasticization of sugars. The sudden increase in the adsorption with the increase of the water activity for the chitosan films is due to this plasticization, reflected in the sudden increase of the active sites that may lead to a break in the polysaccharide crystalline structure. [39]

As concerns the beeswax addition in the films, for every percentage used, the content of absorbed water is very similar until water activities of 0.9. For water activities from 0.9 on, the films without beeswax are clearly more hydrophilic and the hydrophilicity decreases with the increase in beeswax content. The interaction between the chitosan and the beeswax leads to an increase in the number of the hydrophobic particles, that don't interact with water. There are few active sites available for water adsorption in the polymeric matrix due to the arrangement of the lipid chains.

4.6 WATER VAPOUR PERMEABILITY

Water vapour permeability (WVP) is considered a crucial property for films intended to be used as edible food coatings, because most natural biopolymers are very prone to water absorption.

In an ideal polymeric structure, WVP is independent from the film thickness, however there are experimental evidences that this ideal behaviour does not exist. Some studies, made with hydrophilic films concluded that the WVP increases with the films thickness [12] [25] [21] [40] [23] [29] [22]. This deviation from the ideal behaviour indicates the films strong affinity with water, behaviour that is not taken into account by Henry's law [23]. The obtained water vapour isotherms for the studied films in this work, confirm this behaviour. The effect of thickness in WVP is due to the swelling of the film as the result of the attractive forces between the polymer and water. This swelling can result in the variation of the polymer structure, affecting the permeability.

The selection of the driving force was made based in the hydrophilic character of the films material, expressed by the water sorption isotherm. The water entering the films is acting as a diffusion species and as a plasticizer. In this way, it loosens the polymeric matrix and, consequently, water transport is facilitated [25].

The WVP results for Ch and Ch + BW films for a 80.6% - 32.4% RH driving force, are presented in Figure 4.14. WVP slightly decreases as the beeswax content increases, which strengthen the hypothesis of uniform distribution of the beeswax in the plasticized chitosan network. [29]

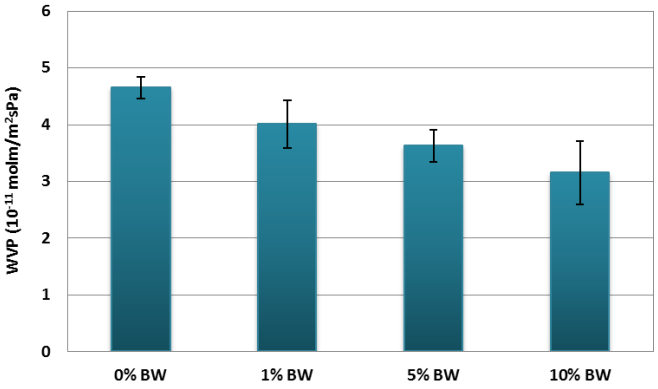

Figure 4.14 – Relation between the WVP and the beeswax content of the films.

The effective diffusion coefficients and solubility coefficients obtained are shown in **Erro! A origem da referência não foi encontrada.**. In Figure 4.15 a decrease of the diffusion coefficients as the beeswax content increases can be noticed.

Table 4.8 - Effective diffusion coefficient and solubility coefficient (Driving force: 80.6 - 32.4 %(RH)).

Film	D_{eff} (10^{-12} m^2/s)	S_2 (mol/m^3Pa)	S_3 (mol/m^3Pa)	$S_2.a_{w2} - S_3.a_{w3}$ (mol/m^3Pa)
Ch	7.24 ± 0.37	3.454	1.378	1.71
Ch + 1% BW	5.51 ± 0.69	3.761	1.525	1.94

Ch + 5% BW	4.55 ± 0.49	4.350	1.672	2.28
Ch + 10% BW	3.89 ± 0.65	4.786	1.768	2.62

Analyzing the sorption coefficients it can be seen that they slightly increased with the increase in the beeswax content what generates an increasing driving force. However, a decreased WVP is noticed, which is a result of the water diffusion coefficient.

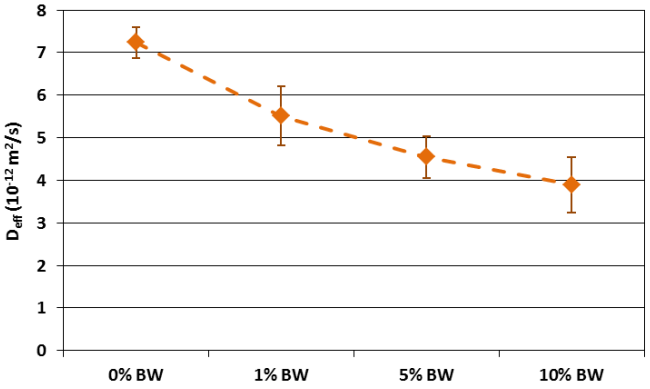

Figure 4.15 – Relation between the diffusion coefficient and the beeswax content of the films.

It is reported in other publications [41] that the addition of a hydrophobic material into an emulsion film does not guarantee reduced WVP, because permeability of emulsion films is influenced not only by the existence of steric hindrance and “tortuosity” for diffusion of water molecules [40] [29] (lowering the diffusion coefficient), but also by the existence of pores, voids, cracks and channellings that may favour water transport [40]. The balance between these two effects originates a decrease of the WVP in a lower extend than it could be expected.

4.7 GAS PERMEABILITY

Most foods require specific atmospheric conditions to keep them fresh and to ensure its preservation as long as possible. To guarantee that the gas composition within the packaging is the most appropriate for a specific product, it is necessary that the packaging material provides certain barrier properties. The most common gases are carbon dioxide, oxygen, nitrogen and a combination of them. Although synthetic polymers present excellent gas barrier properties, the edible films made from biopolymers as proteins and polysaccharides may also exhibit the necessary barrier characteristics.

4.7.1 Carbon dioxide permeability

Carbon dioxide is formed in some food products due to reactions of deterioration and breathing. This gas must be removed from the packaging to prevent spoilage of the food and destruction of the packaging itself. The edible films made from biopolymers can maintain the quality of food and improve their stability and durability, delaying or facilitating the transfer of undesirable

gases (e.g. oxygen or carbon dioxide, respectively) in food products such as fruits and vegetables.

In this experiment, the carbon dioxide permeability of the chitosan and chitosan/beeswax films was studied. The humidity conditions determine the amount of water absorbed by the films, and therefore, the gas permeation. The gas permeability increases significantly as the hydration of the polymeric matrix increases as such. All the samples where conditioned at the same humidity conditions, a_w=0.52.

In Figure 4.16 the evolution of films permeability with the beeswax content can be observed. Comparing the studied films it can be noticed that the chitosan without beeswax addition films show a better carbon dioxide barrier, and the films become more permeable to this gas as the incorporated percentage of beeswax increases. This fact can be attributed to a higher solubility of carbon dioxide in the chitosan/beeswax films. Therefore carbon dioxide permeability is sensitive to changes in the films composition.

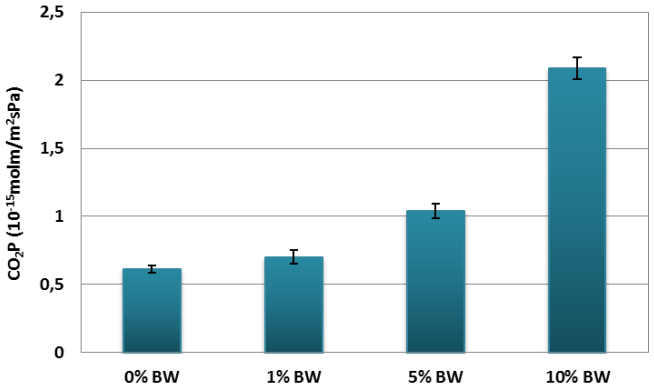

Figure 4.16 – Evolution of the CO_2P with the content of beeswax.

Comparing the CO_2P values obtained with the WVP values we can see that the chitosan films produced impart a much higher barrier to carbon dioxide than to water vapour (with a difference of about 4 orders of magnitude).

In **Erro! A origem da referência não foi encontrada.** some values of CO_2P of films produced from natural and synthetic polymers are shown. The comparison of the presented values cannot be done directly as the films present differences in the hydration and this factor greatly influences the permeability to gases.

Table 4.9 - Comparison of the CO_2P in different films (natural and synthetic).

Film	Plasticizer	%RH	T(ºC)	CO_2P (10^{-15}mol.m/m^{2}sPa)	Reference
Starch	-	100	24	26.41	[42]
EPS	-	43.7	30	0.2	[22]
k-carrageenan/pectin	-	25	30	3.9	[25]
Pectin	-	87	25	21.3	[42]
Chitosan	-	0	25	0.0018	[42]
Chitosan	-	93	25	8.01	[42]
Chitosan	Glycerol(1:1)	50	20	2.43	[43]
Ch	Glycerol(1:0.5)	52	30	0.612	Present work
Ch + 10% BW	Glycerol(1:0.5)	52	30	2.087	Present work
Pullulan	-	30	25	0.072	[42]
Wheat gluten	-	0	25	0.0074	[42]
Wheat gluten	-	91	25	24.5	[42]
Wheat gluten /BW	-	91	25	6.614	[42]
PET	-	0	23	0.038	[42]
PVC	-	0	NR[1]	0.31	[44]
PE	-	0	NR	0.54	[44]
LDPE	-	0	23	4.2	[42]

Comparing the chitosan films prepared without beeswax incorporation with the films prepared with 10% beeswax, we can see that there is an increase in CO_2P. For the wheat gluten films and for the same hydration degree, when there is beeswax incorporation in the films formulation, the values of CO_2P decrease, making them a better barrier to CO_2.

In the wheat gluten case, it can be observed that the barrier capacities show a high variation with the hydration degree of the films. However for high humidities (91% RH) the permeability increases a lot even with the insertion of beeswax in the films. For the chitosan films the incorporation of beeswax increase the CO_2 permeability what makes the chitosan-beeswax emulsion a less effective barrier to carbon dioxide than the wheat gluten-beeswax emulsion, taking into account the different hydration of the films.

In relation to the other natural polymers presented, chitosan is a better barrier to CO_2 than the k-carrageenan/pectin films and the starch films, for the humidity presented, without neglecting that an increase in the films humidity increases its permeability to gases too, as previously referred. The EPS (Exopolysacharyde) films were tested with a similar hydration degree that the chitosan films and present a lower CO_2P, showing themselves as a better barrier to this gas.

Comparing now with the synthetic polymers, it can be seen that the chitosan films are better barriers to CO_2 than the LDPE (low density polyethylene) films. The permeability values for PET (polyethylene terephthalate) and PVC (polyvinyl chloride) films are very similar to permeability values of the chitosan films without beeswax addition. The beeswax addition decreases the barrier properties of the prepared chitosan films to CO_2.

[1] NR – Not reported

4.7.2 Oxygen permeability

Oxygen is the key factor gas that can cause oxidation inducing many unwanted changes in food like odour, colour and taste, and food nutrient deterioration. Therefore films that provide a good oxygen barrier can help improving the quality of food products and enhance its durability.

In this experiment the operation conditions and the conditioning of the films were similar to the ones in the CO_2P essay. The only difference was that the O_2P was only determined for Ch films and for Ch + 10% BW films. In **Erro! A origem da referência não foi encontrada.** the values of O_2P obtained are shown.

Table 4.10 - Oxygen permeability results.

Film	Thickness (μm)	O_2P (10^{-16} mol.m/m^{2}sPa)
Ch	62.30 ± 0.42	2.241 ± 0.238
Ch + 10% BW	65.20 ± 1.70	0.222 ± 0.026

Comparing the obtained values, it can be observed that the chitosan films without the addition of beeswax are about 10 times more permeable to oxygen then the chitosan films that contain 10% of beeswax incorporated in its matrix. This can be explained by the low oxygen solubility in the beeswax films due to its composition characteristics. This makes the chitosan films with 10% of beeswax addition excellent oxygen barriers.

By comparing the oxygen permeability values with the water vapour permeability and carbon dioxide permeability values, it can be seen that the chitosan films produced are a better oxygen barrier then a barrier to the water vapour or the carbon dioxide, whatever its composition.

In **Erro! A origem da referência não foi encontrada.** some oxygen permeability values are presented for films produced with natural and synthetic polymers.

Table 4.11 – Oxygen permeability in different films (biological and synthetic).

Film	Plasticizer	%RH	T(ºC)	O_2P (10^{-16}molm/m^{2}sPa)	Reference
MC	-	52	25	465	[45]
MC/BW	NR	0	25	5	[42]
HPMC	-	50	24	1406	[45]
Starch	-	57	20	7.25	[46]
Starch	Sorbitol (4:1)	57	20	1.65	[46]
Chitosan	NR	0	25	0.006	[42]
Chitosan	NR	93	25	4.72	[42]
Chitosan	-	50	25	170	[47]
Chitosan	Glycerol(1:1)	50	20	2.23	[43]
Chitosan	Glycerol (1:0.3)	50	23	1.97	[48]
Ch	Glycerol (1:0.5)	52	30	2.24	Present work
Ch + 10% BW	Glycerol (1:0.5)	52	30	0.22	Present work
Zein	Glycerol (2.6:1)	0	25	202 – 465	[45]
Gluten	Glycerol (2.5:1)	0	25	31.5	[45]
SPI	Glycerol (2.4:1)	0	25	31.5	[45]
WPI	Sorbitol (2.3:1)	50	23	22.2	[45]
Collagen	-	0	RT[2]	0.21 – 2.58	[45]
Collagen	-	63	RT	119	[45]
PET	-	NR	NR	67.2	[49]
LDPE	-	50	23	9665	[45]
HDPE	-	50	23	2207	[45]
Polyester	-	50	23	80.63	[45]
PE	-	50	25	97.17	[50]
PP	-	50	25	13.96	[50]

Oxygen permeability of the chitosan films produced is generally better than that of the other films presented in the table. The chitosan films with beeswax incorporation can be 10 times less permeable than the collagen films (conditioned at 0%RH) and more than 1000 times in relation to the MC films (conditioned at 52%RH). Regarding the synthetic polymers presented, all of them show week barrier characteristics regarding oxygen. For the MC films presented on the table oxygen permeability decreased about 90 times with the beeswax addiction. On the contrary, for the Ch films studied in this work the beeswax incorporation reduced the O_2P in about 10 times, what revealed an important improvement in the films.

It is possible to see and confirm that the %RH as a high influence on gas permeability. For example for the chitosan films in the same study permeability measured at different %RH have very different results, at low %RH the permeability is much lower than at high %RH values. For the collagen films the same behaviour was observed.

Other determinant parameter in the permeability is the composition of the films, as it can be seen for the different chitosan films presented in the table with the same %RH imposed, the permeability values range from $1.97 \times 10^{-16}\, molm/m^2 sPa$ to $170 \times 10^{-16}\, molm/m^2 sPa$, differences that can be explained with the different content of plasticizers, surfactants and even the chitosan type.

[2] RT – room temperature

4.7.3 Selectivity

The selectivity, represented by the carbon dioxide/oxygen permeability ratio, is one of the most descriptive parameters of a film and determines the relative proportions of carbon dioxide and oxygen in the package. Films with high ratio values will allow carbon dioxide to escape from the package relatively easily, resulting in low carbon dioxide concentration atmosphere. Films with lower ratio values will allow greater CO_2 build-up in the package. The selectivity ratio determines the possible combination of oxygen and carbon dioxide concentrations inside the film. Since fruits and vegetables vary in their tolerance to carbon dioxide and in their ability to benefit from high percentages of this gas, the selectivity ratio value of a film is very important for predicting the relative amounts of oxygen and carbon dioxide that will accumulate. [42]

In Table 4.12 the gas selectivity coefficient of various films (bio-based and synthetic) are presented for comparison.

Table 4.12 - Gas selectivity coefficient (carbon dioxide/oxygen permeability ratio) of various films.

Film	Plasticizer	%RH	Gas selectivity coefficient	Reference
Pectin	-	96	16.0	[42]
Chitosan	-	93	17.0	[42]
Chitosan	Glycerol (1:1)	50	10.9	[43]
Ch	Glycerol (1:0.5)	52	2.7	Present work
Ch + 10% BW	Glycerol (1:0.5)	52	94	Present work
Pullulan	-	30	4.2	[42]
Wheat gluten	-	91	25.0	[42]
Wheat gluten/BW	-	91	9.6	[42]
PVC	-	50	5.8	[42]
PP	-	50	4.0	[42]

The selectivity values decreased when lipid components were added to wheat gluten, but the ratio obtained remained more than twice as high as in common synthetic films. Despite the selectivity coefficient value for the Ch films studied in this work is very low comparing to the other chitosan films presented in the table, the selectivity increased from 2.7 to 94 with the lipid addiction which represents a major improvement in the films selectivity. Comparing to the synthetic polymer films the Ch films studied in this work have a very low selectivity, about half of the value, which did not happen with the other biopolymer-based films presented in the table that have more than double the selectivity of the synthetic ones.

The %RH, especially for the hydrophilic films represented, greatly influences the permeability and as so the selectivity coefficient, as such it is difficult to compare the obtained values with the literature ones. Besides this condition the composition of the films also influences these parameters.

5 CONCLUSIONS AND FUTURE WORK

5.1 CONCLUSIONS

In the present study edible chitosan and chitosan-beeswax emulsion films were prepared. All the obtained films were transparent with a slightly yellowish colour what lead to the realization of colour alteration and transparency tests. It was verified that the films decrease the original colour intensity of coloured paper, but maintained the hue. The colour alteration imposed by the chitosan and chitosan-beeswax films is visible by the human eye since $\Delta E > 3$ and the colour alteration although small, is significant.

From the contact angle measurements with glycerol, films surface have shown an increase of their surface hydrophobicity with the inclusion of beeswax in the chitosan matrix. This fact was shown by higher contact angle values and lower contact angle changes over time, measured on the wax containing films.

SEM images of the films surface revealed that all the films are homogeneous and dense. However the cross-section images of the films with beeswax incorporation presented some structural discontinuities, which were more pronounced as the beeswax content increased. Nevertheless any pores or holes were detected in the structure.

The inclusion of beeswax into the chitosan matrix led to a decrease of both Young modulus and tension at break, indicating that the wax may have act as plasticizer originating less rigid films. However, the toughness of the films as decreased, as shown by the lower elongation at break, either under tensile or puncture tests. This fact is attributed to the discontinuities created by the solid wax particles within the chitosan matrix.

Relatively to the hygroscopic properties it was found that the best model for describing the water sorption isotherms of all the films was the GAB model, with a typical behaviour of polysaccharide constituted materials. The water sorption increased identically for all the films as the water activity increased – for aw values below 0.8. Above this value, the films with 5% and 10% beeswax content presented lower water adsorption capacity.

A decrease of the water vapour permeability with increasing beeswax content was observed. For the studied driving force the water vapour permeability decreased from $4.647 \times 10^{-11}\, mol.m/m^2.s.Pa$ for the chitosan without beeswax films, to $3.159 \times 10^{-11}\, mol.m/m^2.s.Pa$ for the chitosan with 10% beeswax content. This decrease was expected and it is due to the reduction of the films hydrophilicity and to the decrease of the effective water diffusion coefficient caused by the solid beeswax particles within the chitosan matrix.

The carbon dioxide and oxygen permeabilities were also determined. While an increase of the carbon dioxide permeability was observed (from $6.12 \times 10^{-16}\, mol.m/m^2.s.Pa$ for the chitosan without beeswax films to $2.087 \times 10^{-15}\, mol.m/m^2.s.Pa$ for the chitosan with 10% beeswax content), the oxygen permeability strongly decreased (from $2.241 \times 10^{-16}\, mol.m/m^2.s.Pa$ for the chitosan without beeswax films to $2.22 \times 10^{-17}\, mol.m/m^2.s.Pa$ for the chitosan with 10% beeswax content), achieving a carbon dioxide permeability/oxygen permeability ratio of 94. This value is quite interesting for applications where a good CO_2 (product of the respiration process) permeation is desired, preventing at the same time the permeation of O_2 that can cause the oxidation of the coated products.

In an overall conclusion it can be said that the studied films show great potential in the food industry for edible and biodegradable coatings. In the majority of the parameters studied in this work the introduction of beeswax improved the chitosan films characteristics. Further studies should be focused on promoting a better homogenization of the wax in the polymer matrix, in order to improve the barrier properties to water vapour.

5.2 FUTURE WORK

This work contributed to a better understanding of the edible and biodegradable chitosan and chitosan-beeswax emulsion films in what concerns their optical, superficial, structural, mechanical, hygroscopic and barrier properties. However there are still some aspects that can be studied in further research.

- → The optimization of the emulsion forming and stabilization process in order to create more disperse and homogeneous wax/chitosan matrices;
- → New formulation of the emulsion films with percentages ranging between 5% and 10% content of beeswax;
- → Gas permeability studies with gas mixtures;
- → The study of the biodegradability of the films in aqueous and solid environments;
- → The addition of crosslinkers to enhance the mechanical and structural properties;
- → The application of the films in fresh fruits and vegetable in order to study the behavior of the films when applied as edible coatings.

6 REFERENCES

[1] M. E. Embuscado e K. C. Huber, Edible Films and Coatings for Food Aplications, Springer, 2009.

[2] J.-W. Rhim e P. K. W. Ng, "Natural Biopolymer-Based Nanocomposite Films for Packaging Applications, Critical Reviews," *Food Science and Nutrition (2007),* vol. 47, n.º 4, pp. 411-433.

[3] S. R. Kanatt, M. S. Rao e A. S. S. P. Chawla, "Active chitosan-polyvinyl alcohol films with natural extracts," *Food Hydrocolloids (2012),* vol. 29, pp. 290-297.

[4] S. A. Valencia-Chamorro, L. Palou, M. A. d. Río e M. B. Pérez-Gago, "Antimicrobial Edible Films and Coatings for Fresh and Minimally Processed Fruits and Vegetables: A Review," *Food Science and Nutricion - Critical Reviews (2011),* vol. 51, n.º 9, pp. 872-900.

[5] K. D. Vu, R. G. Hollingsworth, E. Leroux, S. Salmieri e M. Lacroix, "Development of edible bioactive coating based on modified chitosan for increasing the shelf life of strawberries," *Food Research International (2011),* vol. 44, pp. 198-203.

[6] M. Aider, "Chitosan application for active bio-based films production and potencial in the food industry: review," *LWT - Food Science and Technology (2010),* vol. 43, pp. 837-842.

[7] V. Falguera, J. P. Quintero, A. Jiménez, J. A. Munoz e A. Ibarz, "Edible films and coatings: Structures, active functions and trends in their use," *Trends in Food Science & Technology (2011),* vol. 22, pp. 292-303.

[8] M. Flieger, M. Kantorová, T. R. A. Prell e J. Votruba, "Biodegradable plastics from renewable sources," *Folia Microbiol. (Praha) (2003),* vol. 48, pp. 27-44.

[9] B. W. Souza, "Characterization of new hydrocolloids to be used as food coatings and integration of their application with ohmic heating," Tese de Doutoramento em Engenharia Química e Biológica, Universidade do Minho - Escola de Engenharia, Setembro 2010.

[10] B. K. Tiwari, V. P. Valdramidis, K. M. Colm P. O'Donnell, P. Bourke e P. Cullen, "Application of Natural Antimicrobials for Food Preservation," *Journal of Agriculture and food Chemistry - Review (2009),* vol. 57, pp. 5987-6000.

[11] P. C. Srinivasa e R. N. Tharanathan, "Chitin/Chitosan - Safe, Ecofriendly Packaging Materials with Multiple Potential Uses," *Food Reviews International (2007),* vol. 23, n.º 1, pp. 53-72.

[12] G. A. Morris, J. Castile, A. Smith, G. G. Adams e S. E. Harding, "Macromolecular Conformation of Chitosan in Dilute Solutions: A New Global Hydrodynamic Approach," *Carbohydrate Polymers (2009),* vol. 76, pp. 616-621.

[13] M. A. Garcia, M. N. Martino e N. E. Zaritzky, "Lipid addition to improve barrier properties of edible starch-based films and coatings," *Journal of Food Science (2000),* vol. 65, pp. 941-947.

[14] C. Han, C. Lederer, M. McDaniel e Y. Zhao, “Sensory evaluation of fresh strawberries (Fragaria ananassa) coated with chitosan-based edible coatings,” *Journal of Food Science (2005),* vol. 70, pp. 172-180.

[15] M. N. Belgacem e A. Gandini, Monomers, Polymers and Composites from Renewable Resources, Elsevier, 2008.

[16] V. Morillon, F. Debeaufort, G. Bond, M. Capelle e A. Voilley, “Factors affecting the moisture permeability of lipid-based edible films: A review.,” *Critical Reviews in Food Science and Nutrition (2002),* vol. 42, n.º 1, pp. 67-89.

[17] T. H. Shellhammer e J. M. Krochta, “Whey protein emulsion film performance as affected by lipid type and amount,” *Journal of Food Science (1997),* vol. 62, n.º 2, pp. 390-394.

[18] T. Karbowiak, F. Debeaufort e A. Voilley, “Influence of thermal process on structure and functional properties of emulsion-based edible films,” *Food Hydrocolloids (2007),* vol. 21, pp. 879-888.

[19] M. B. Perez-Gago e J. M. Krochta, “Emulsion and bi-layer edible films,” *Innovations in Food Packaging (2005).*

[20] E. Bouyera, G. Mekhloufia, V. Rosilio, J.-L. Grossiorda e F. Agnelya, “Proteins, polysaccharides and their complexes used as stabilizers for emulsions: Alternatives to synthetic surfactants in the pharmaceutical field? - Review,” *International Journal od Pharmaceutics (2012),* vol. 436, pp. 359-378.

[21] M. A. Bertuzzi, E. F. C. Vidaurre, M. Armada e J. C. Gottifredi, “Water vapor permeability of edible starch based films,” *Journal of Food Engineering (2007),* vol. 80, pp. 972-978.

[22] M. J. Fabra, P. Talens e A. Chiralt, “Tensile properties and water vapor permeability of sodium caseinate films containing oleic acid-beeswax mixtures,” *Journal of Food Engineering (2008),* vol. 85, pp. 393-400.

[23] S. Y. Quek, N. K. Chok e P. Swedlund, “The physicochemical properties of spray-dried watermelon powders,” *Chemical Engineering and Processing: Process Intensification (2007),* vol. 46, n.º 5, pp. 386-392.

[24] L. C. Chaves, “Estudo da Cinética de Formação de Biofilmes em Superficies em Contacto com Água Potável,” Dissertação apresentada para obtenção do grau de mestre em tecnologia do ambiente, Universidade do Minho - Departamento de Engenharia Biológica, 2004.

[25] V. D. Alves, N. Costa e I. M. Coelhoso, “Barrier properties of biodegradable composite films on kappa-carrageenan/pectin blends and mica flakes,” *Carbohydrate Polymers (2010),* vol. 79, pp. 269-276.

[26] T. Rodrigues, “Preparação e Caracterização de Membranas Biodegradáveis,” Dissertação para obtenção do Grau de Mestre em Engenharia Química e Bioquímica - FCT/UNL, Lisboa, 2008.

[27] V. D. Alves, A. R. Ferreira, N. Costa, F. Freitas, M. A. Reis e I. M. Coelhoso, “Characterization of biodegradable films from the extracellular polysaccharide produced by

Pseudomonas oleovorans grown on glycerol byproduct," *Carbohydrate Polymers (2011),* vol. 83, pp. 1582-1590.

[28] J. S. Wang, J. P. Derocher, L. F. Wu, F. S. Bates e E. L. Cussler, "Barrier films made with various lamellar block copolymers," *Journal of Membrane Science (2006),* vol. 270, pp. 13-21.

[29] M. Pereda, G. Amica e N. E. Marcovich, "Development and characterization of edible chitosan/olive oil emulsion films," *Carbohydrate Polymers (2012),* vol. 87, pp. 1318-1325.

[30] S.-I. Hong, J. H. Han e J. M. Krochta, "Optical and surface properties of whey protein isolate coatings on plastic films as influenced by substrate, protein concentration, and plasticizer type," *Journal of Applied Polymer Science (2004),* vol. 92, pp. 335-343.

[31] M. Vargas, A. Albors, A. Chiralt e C. González-Martínez, "Characterization of chitosan-oleic acid composite films," *Food Hydrocolloids (2009),* vol. 23, pp. 536-547.

[32] R. Villalobos, J. Chanona, P. Hernandez, G. Gutierrez e A. Chiralt, "GIoss and transparency of hydroxypropylmethylcellulose films containing surfactants as affected by their microstructure," *Food Hydrocolloids (2005),* vol. 19, pp. 53-61.

[33] M. Pereda, A. G. Ponce, N. E. Marcovich, R. A. Ruseckaite e J. F. Martucci, "Chitosan-gelatin composites and bi-layer films with potencial antimicrobial activity," *Food Hydrocolloids (2011),* vol. 25, pp. 1372-1381.

[34] M. L. Navarro-Tarazaga, R. Sothornvit e M. B. Pérez-Gago, "Effect of plasticizer type and amount on hydroxypropil methylcellulose-beeswax edible film properties and postharvest quality of coated plums (cv. Angeleno)," *Journal of Agricultural and Food Chemistry (2008),* vol. 56, pp. 9502-9509.

[35] M. Soazo, A. C. Rubiolo e R. A. Verdini, "Effec of drying temperature and beeswax content on physical properties of whey protein films," *Food Hydrocolloids (2011),* vol. 25, pp. 1251-1255.

[36] A. R. V. Ferreira, "Preparação e carcaterização de filmes obtidos a partir de biopolímeros microbianos," Dissertação para obtenção do Grau de Mestre em Engenharia Química e Bioquímica - FCT/UNL, Lisboa, 2010.

[37] OriginLab, *Origin 8 help files,* Northampton, MA: Origin, 2007.

[38] S. Ludwiczak e M. Mucha, "Modeling of water sorption isotherms of chitosan blends," *Carbohydrate Polymers (2010),* vol. 79, pp. 34-39.

[39] K. O. Falade e O. C. Aworh, "Adsorption isotherms of osmo-oven dried African star apple (Chrysophyllum albidum) and African mango (Irvingia gabonensis) slices," *European Food Research and Technology (2004),* vol. 218, pp. 278-283.

[40] L. H. Cheng, A. Karim e C. C. Seow, "Characterization of composite films made of konjac glucomannan (KGM), carboxymethyl cellulose (CMC) and lipid," *Food Chemistry (2008),* vol. 107, pp. 411-418.

[41] P. C. Srinivasa, M. N. Ramesh e R. N. Tharanathan, "Effect of plasticizers and fatty acids

on mechanical and permeability characteristics of chitosan films," *Food Hydrocolloids (2007),* vol. 21, pp. 1113-1122.

[42] N. Gontard, R. Thibault, B. Cuq e S. Guilbert, "Influence of relative humidity and film composition on oxygen and carbon dioxide permeabilities of edible films," *Journal of Agricultural and Food Chemistry (1996),* vol. 44, pp. 1064-1069.

[43] P. Fajardo, J. T. Martins, C. Fucinos, L. Pastrana, J. A. Teixeira e A. A. Vicente, "Evaluation of a chitosan-based edible film as carrier of natamycin to improve the storability of Saloio cheese," *Journal of Food Engineering (2010),* vol. 101, pp. 349-356.

[44] H. J. Park, "Development of advanced sdible coatings for fruits - review," *Trends in Food Science & Technology (1999),* vol. 10, pp. 254-260.

[45] K. S. Miller e J. M. Krochta, "Oxygen and aroma barrier properties of edible films: a review," *Trends in Food Science and Technology (1997),* vol. 8, pp. 228-237.

[46] S. Gaudin, D. Lourdin, D. Le Botlan, J. L. Ilari e P. Colonna, "Plasticisation and mobility in starch-sorbitol film," *J. Cereal Sci.(1999),* vol. 29, pp. 273-284.

[47] P. Di Pierro, A. Sorrentino, L. Mariniello e C. V. L. Giosafatto, "Chitosan/whey protein film as active coating to extend Ricotta cheese shelf-life," *LWT - Food Science and Technology (2011),* vol. 44, pp. 2324-2327.

[48] I. Leceta, P. Guerrero e K. de la Caba, "Funcional properties of chitosan-based films - http://dx.doi.org/10.1016/j.carbpol.2012.04.031," *Carbohydrate Polymers (2012).*

[49] J. H. Han e J. M. Krochta, "Physical properties of whey protein coating solutions and films containing antioxidants," *J. Food Science (2007),* vol. 72, n.º 5, pp. 308-314.

[50] S. I. Hong e J. M. Krochta, "Oxygen Barrier Performance of Whey Protein Coated Plastic films as Affected by Temperature, Relative Humidity, Base film and Protein Type," *Journal of Food Engineering (2006),* vol. 77, pp. 739-745.

[51] V. D. Alves e I. M. Coelhoso, "Orange juice concentration by osmotic evaporation and membrane distillation: A comparative study," *Journal of Food Engineering (2006),* vol. 74, pp. 125-133.

[52] K. Chinabhark, S. Benjakul e T. Prodpran, "Effect of pH on the properties of protein-based film from bigeye snapper (Picanthus tayenus) surimi," *Bioresource Technology (2007),* vol. 98, pp. 221-225.

[53] M. Kong, X. G. Chen, K. Xing e H. J. Park, "Antimicrobial properties of chitosan and mode of action: A state of the art review," *International Journal of Food Microbiology (2010),* vol. 144, pp. 51-63.

7 ANNEXES

ANNEX I. B PARAMETER CALCULATION

In the calculation of β parameter, a PDMS membrane was used due to its well-known permeability. The test gas used was nitrogen. From the pressure data obtained in each permeation cell (feed and permeate) over the time, the graphics in Figure 7.1 were traced.

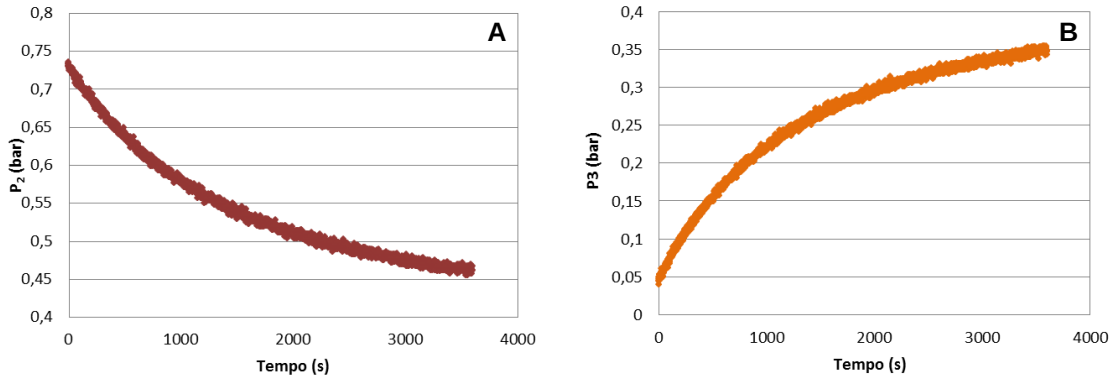

Figure 7.1 – Representation of the pressure over the time for the β calculation essay. (A – Feed; B – Permeate).

By modifying the Equation 3.30 and making it a linear equation where the slope turns into the beta parameter, the next expression is obtained:

$$\frac{1}{P}\ln\left(\frac{\Delta P_0}{\Delta P}\right) = \beta\frac{t}{\delta}$$

Using the nitrogen permeability value for the PDMS membrane referred in the bibliography, the graphic of $\frac{1}{P}\ln\left(\frac{\Delta P_0}{\Delta P}\right)$ versus $\frac{t}{\delta}$ were traced and from where β value (slope) is taken (Figure 7.2).

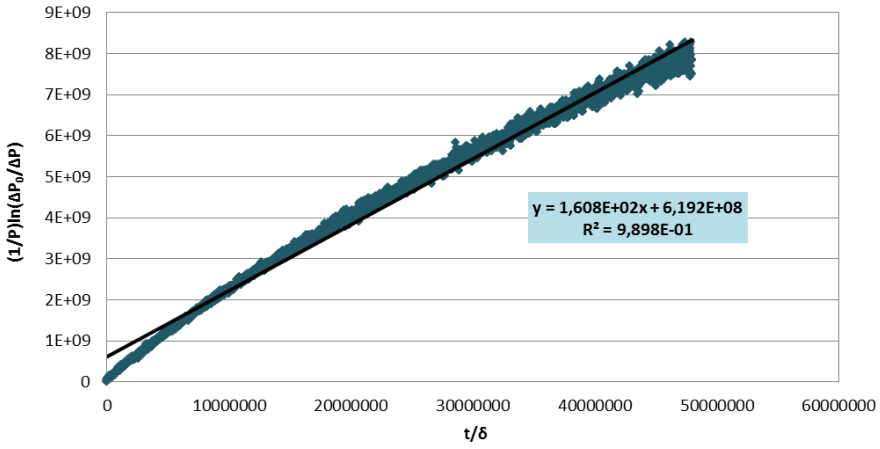

Figure 7.2 – Graphical representation of the experimental data where the β parameter is taken from the slope of the tendency line.

ANNEX II. TRANSPARENCY AND CONTACT ANGLE

The transparency was calculated by determining the transmittance logarithm coefficient at 600 nm by the films thickness. In Table 7.1 the experimental values used to make this calculation are presented.

Table 7.1 - Experimental values used to calculate the films transparency.

Films	Sample	Thickness (µm)	Absorbance	Transmittance	Transparency
Ch	1	67.25	0.065	0.861	0.966
	2	60.75	0.070	0.851	1.152
	3	53.50	0.067	0.857	1.252
	4	57.00	0.079	0.834	1.386
	5	74.25	0.072	0.847	0.969
	6	76.00	0.081	0.830	1.066
Ch + 1%BW	7	65.75	0.097	0.800	1.475
	8	89.75	0.109	0.778	1.214
	9	55.00	0.102	0.791	1.855
	10	89.75	0.110	0.776	1.226
	11	81.50	0.131	0.740	1.607
	12	83.00	0.126	0.748	1.518
Ch + 5%BW	13	75.00	0.136	0.731	1.813
	14	45.75	0.118	0.762	2.579
	15	49.00	0.119	0.760	2.428
	16	99.75	0.103	0.789	1.033
Ch + 10%BW	17	59.25	0.183	0.656	3.089
	18	74.25	0.247	0.566	3.327
	19	84.50	0.127	0.746	1.503
	20	58.25	0.123	0.753	2.112

Table 7.2 - Transparency and thickness of the films.

Films	Transparency	Thickness (µm)
Ch	1.132 ± 0.166	64.79 ± 9.23
Ch + 1% BW	1.475 ± 0.242	77.46 ± 14.08
Ch + 5% BW	1.963 ± 0.703	67.38 ± 25.24
Ch + 10% BW	2.507 ± 0.851	69.06 ± 12.63

Table 7.3 - Average contact angle and thickness of the films.

Films	Thickness (µm)	Contact angle (º)
Ch	65 ± 3.5	16.1 ± 2.1
Ch + 1% BW	62.5 ± 2.1	67.7 ± 2.9
Ch + 5% BW	60.9 ± 3.3	82.1 ± 4.2
Ch + 10% BW	63 ± 2.0	51.9 ± 8.7

ANNEX III. MECHANICAL PROPERTIES

For the Young modulus calculation, a selection of the elastic region of the stress-strain curves was made. This region of the curves is linear and the slope represents the Young modulus. In Figure 7.3 are graphics of the elastic region is shown for the used samples of the films.

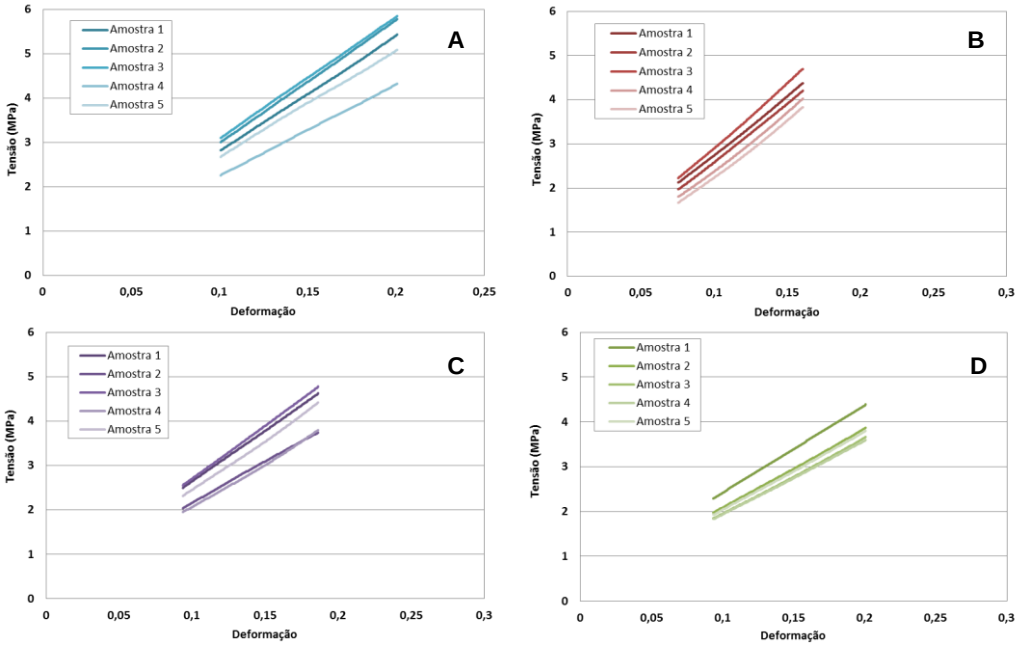

Figure 7.3 – Stress/strain charts from the tensile test – elastic part of the curves – for determination of the Young modulus. (A – Ch films; B – Ch+1%BW films; C – Ch+5%BW films; D – Ch+10%BW films).

ANNEX IV. WATER SORPTION ISOTHERMS

The best fitting model for de sorption isotherms was the GAB model, however other models were adjusted. The following tables (7.1 to 7.5) and figures (7.1 to 7.5) show the obtained parameters and graphics adjusted with the Oswin, Halsey, C&I, Kuhn and Smith models.

Table 7.4 - Parameter values for the Oswin model.

	Film	C	k	$R^2_{ajusted}$	$X^2_{reduced}$
Oswin	Ch	0.0933 ± 0.0101	0.5449 ± 0,0317	0.99164	5.59×10^{-4}
	Ch + 1%BW	0.0985 ± 0.0084	0.5031 ± 0,0260	0.98625	5.51×10^{-4}
	Ch + 5%BW	0.1056 ± 0.0137	0.4268 ± 0,0416	0.9494	1.35×10^{-3}
	Ch + 10%BW	0.0955 ± 0.0142	0.4611 ± 0.0457	0.94981	1.45×10^{-3}

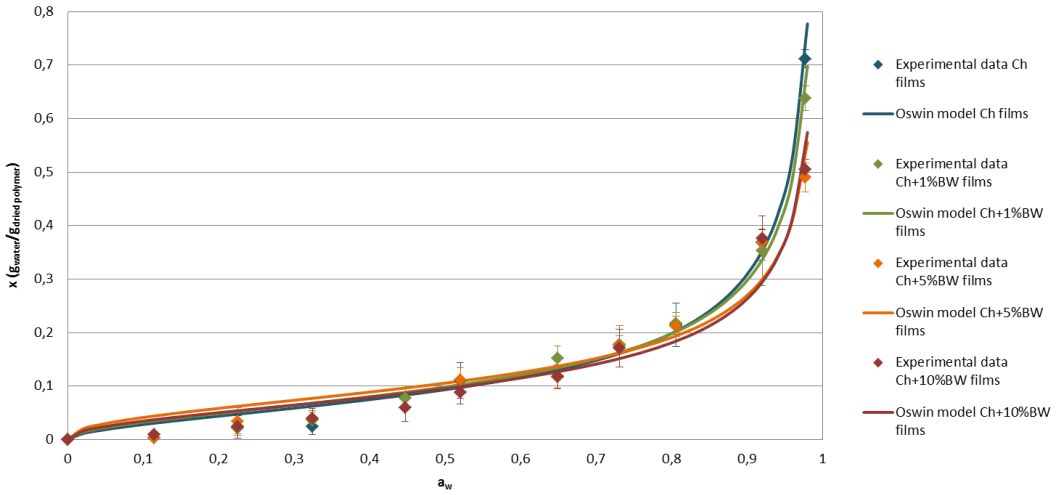

Figure 7.4 – Graphical representation of the water sorption isotherms for the Oswin model.

Table 7.5 - Parameter values for the Halsey model.

	Film	C	k	$R^2_{ajusted}$	$X^2_{reduced}$
Halsey	Ch	0.0782 ± 0.0126	-0.5918 ± 0.0472	0.9835	1.10×10^{-3}
	Ch + 1%BW	0.0816 ± 0.0108	-0.5538 ± 0.0404	0.9711	1.16×10^{-3}
	Ch + 5%BW	0.0892 ± 0.0154	-0.4723 ± 0.0554	0.9231	2.06×10^{-3}
	Ch + 10%BW	0.0789 ± 0.0153	-0.5120 ± 0.0598	0.9275	2.09×10^{-3}

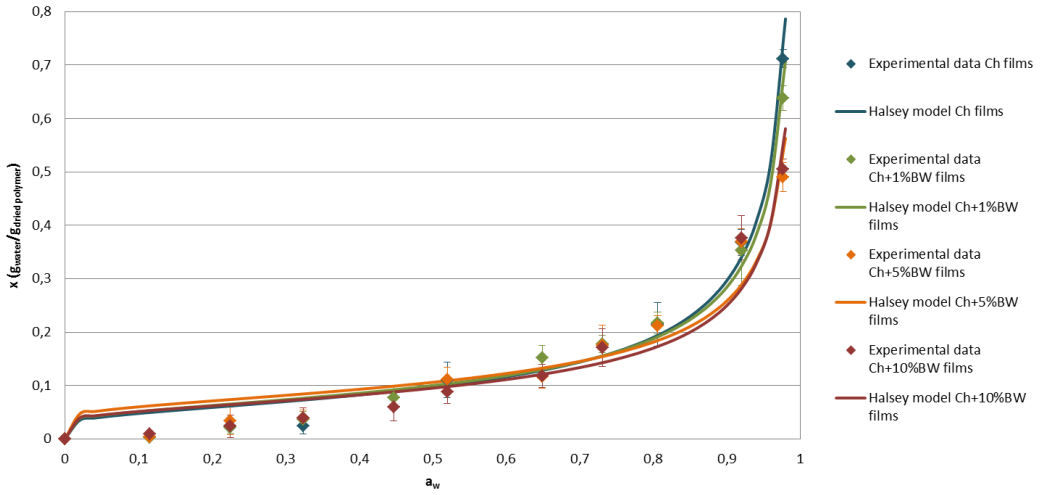

Figure 7.5 - Graphical representation of the water sorption isotherms for the Halsey model.

Table 7.6 - Parameter values for the C&I model

	Film	C	k	$R^2_{ajusted}$	$X^2_{reduced}$
C&I	Ch	0.0694 ± 0.0350	0.0160 ± 0.0021	0.9052	6.34×10^{-3}
	Ch + 1%BW	0.0756 ± 0.0267	0.0143 ± 0.0019	0.8593	5.64×10^{-3}
	Ch + 5%BW	0.0848 ± 0.0306	0.0108 ± 0.0022	0.7247	7.36×10^{-3}
	Ch + 10%BW	0.0685 ± 0.0283	0.0115 ± 0.0020	0.7764	6.44×10^{-3}

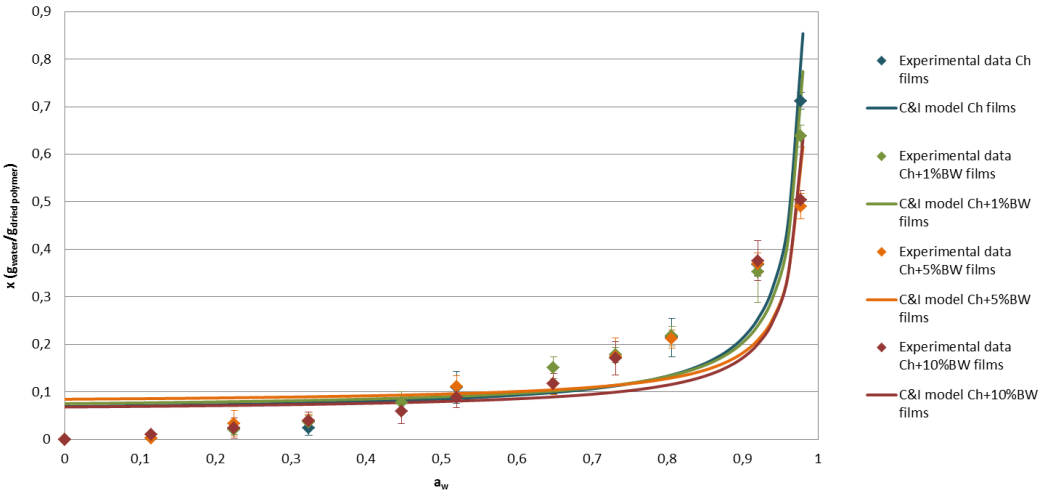

Figure 7.6 - Graphical representation of the water sorption isotherms for the C&I model.

Table 7.7 - Parameter values for the Kuhn model.

	Film	C	k	$R^2_{ajusted}$	$X^2_{reduced}$
Kuhn	Ch	0.0798 ± 0.0353	0.0155 ± 0.0019	0.9245	5.05×10^{-3}
	Ch + 1%BW	0.0806 ± 0.0266	0.0139 ± 0.0018	0.8818	4.74×10^{-3}
	Ch + 5%BW	0.0926 ± 0.0306	0.0104 ± 0.0020	0.7658	6.26×10^{-3}
	Ch + 10%BW	0.0734 ± 0.0288	0.0112 ± 0.0019	0.8017	5.72×10^{-3}

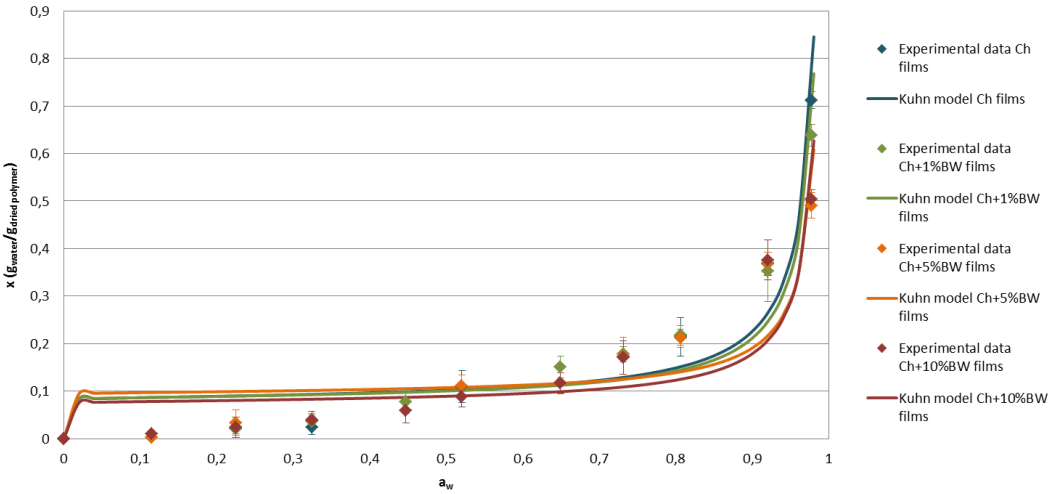

Figure 7.7 - Graphical representation of the water sorption isotherms for the Kuhn model.

Table 7.8 - Parameter values for the Smith model.

	Film	C	k	$R^2_{ajusted}$	$X^2_{reduced}$
Smith	Ch	-0.0366 ± 0.0253	-0.1830 ± 0.0137	0.9675	2.17×10^{-3}
	Ch + 1%BW	-0.0246 ± 0.0111	-0.1648 ± 0.0068	0.9849	6.04×10^{-4}
	Ch + 5%BW	-0.0051 ± 0.0075	-0.1356 ± 0.0046	0.9898	2.73×10^{-4}
	Ch + 10%BW	-0.0124 ± 0.0067	-0.1408 ± 0.0043	0.9917	2.40×10^{-4}

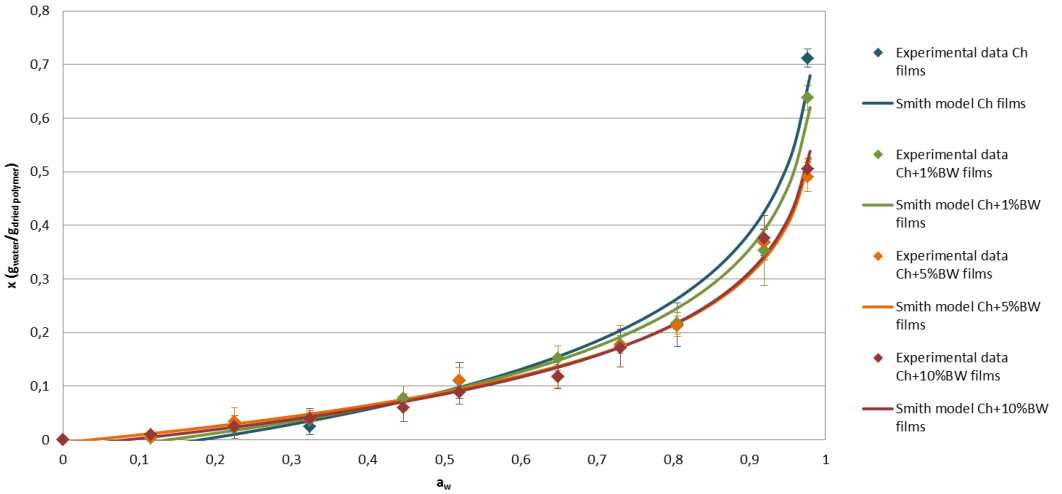

Figure 7.8 - Graphical representation of the water sorption isotherms for the Smith model.

ANNEX V. WATER VAPOUR PERMEABILITY

In the water vapour permeability results treatment, the graphic (Figure 7.9) with the wheight of lost water versus the time of the essay (8.5 hours) was represented. The slope of the adjusted tendency lines correspond do the flow rate of evaporated water (Q_{evap}). In this annex the calculations for the chitosan films without any adittion of beeswax (Ch films) are represented once the calculation method is the same for the other flms.

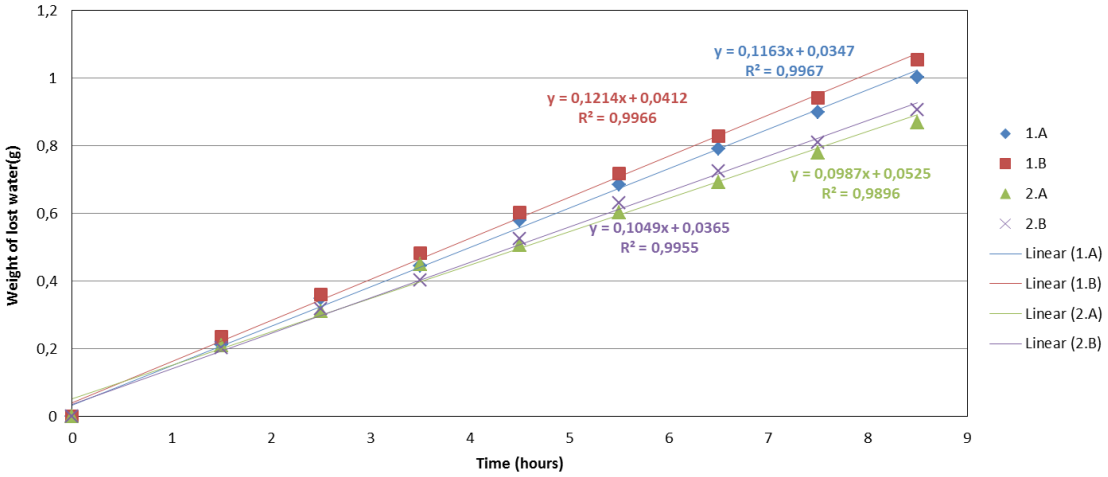

Figure 7.9 – Graphical representation of the weight of lost water versus the time of essay and adjusted tendency lines.

In Table 7.9 the parameter values calculated for each film in order to obtain the water vapour permeability are represented. In Table 7.10 are represented the theoretical parameters used.

Table 7.9 - Calculated parameters used in the WVP determination.

Film	δ (10^5 m)	Q_{evap} (g/h)	N_w (10^4mol/m^{2}s)	V_{evap} (10^{-7}m^3)	H_{evap} (10^{-4}m)	Z_f (10^{-3}m)	Z (10^{-3}m)	y_2 (10^{-2})
1.A	5.9	0.116	9.14	9.89	5.04	7.4	7.17	2.7
1.B	5.8	0.121	9.54	10.3	5.26	7.4	7.18	2.7
2.A	6.1	0.099	7.76	8.39	4.27	10.8	10.6	2.6
2.B	6.3	0.105	8.24	8.91	4.54	10.9	10.6	2.5

Table 7.10 - Theoretical parameters used in the WVP determination.

M_w (g/mol)	R (m^{3}Pa/Kmol)	$P^*_{30^o}$ (Pa)	a_{w1}	a_{w3}	P_{w1} (Pa)	P_{w3} (Pa)	ρ (kg/m^3)
18	8.314	4220	0.806	0.324	3329.9	1505.6	772.11

For the sorption coefficient calculation (S_2 and S_3) the first step was the calculation of the water activity at the membrane surface that due to the mass transfer resistance is not equal to the salt solution water activity imposed. In Figure 7.10 the GAB isotherm for the Ch films and the tangents in the water activity zones in both sides of the film is represented. In Figure 7.10 the calculated values of vapour pressure and water activity at the surface of the films is presented.

From these results the sorption coefficient and the effective diffusion coefficient, which values are presented in the same table, were calculated

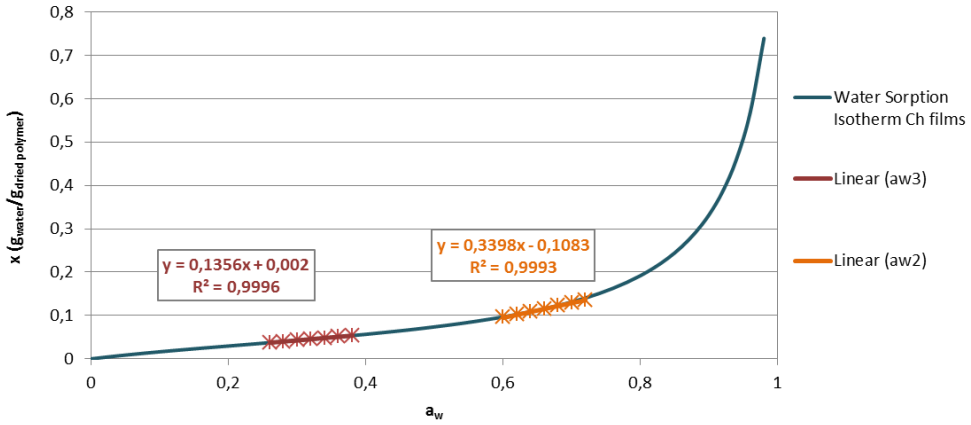

Figure 7.10 – Water sorption isotherm and tangents according to the imposed driving-force.

Table 7.11 - Vapour pressure, water activity and effective diffusion coefficient at the surface of each Ch film.

Film	P_{w2} (Pa)	a_{w2}	Def (m^2/s)
1.A	2727.96	0.646	7.24×10^{-12}
1.B	2700.37	0.640	5.52×10^{-12}
2.A	2571.57	0.609	4.55×10^{-12}
2.B	2523.34	0.598	3.89×10^{-12}

Table 7.12 - WVP and thickness for chitosan and chitosan/beeswax films.

Film	Thickness (μm)	WVP (10^{-11} mol.m/m^2sPa)
Ch	60.3 ± 1.5	4.647 ± 0.195
Ch + 1% BW	57.9 ± 1.7	4.008 ± 0.415
Ch + 5% BW	60.9 ± 2.5	3.624 ± 0.288
Ch + 10% BW	60.7 ± 2.4	3.159 ± 0.557

ANNEX VI. GAS PERMEABILITY

Through the software LabView acquired data, the pressure in both cells (feed and permeate) over the time was obtained and then graphically represented. In Figure 7.11 this graphical representation for one sample of the Ch films is presented. For the remaining films and gases the used method was the same.

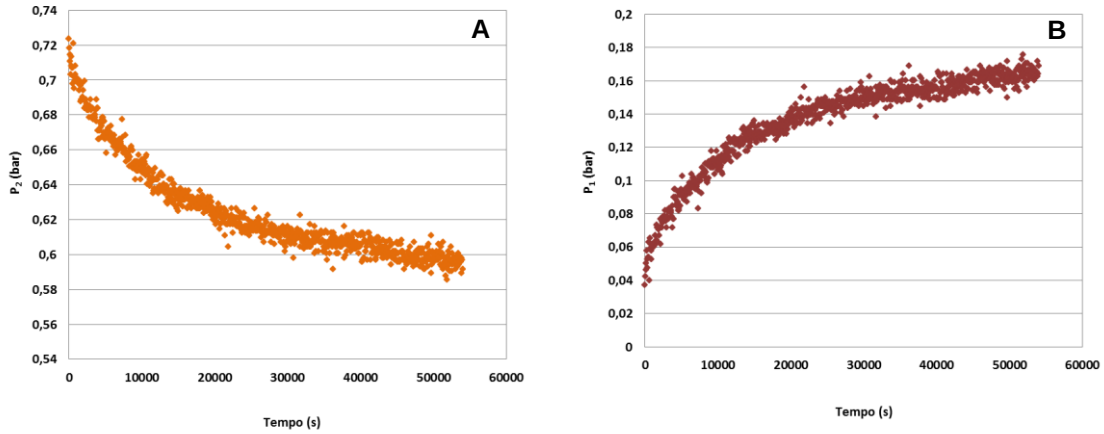

Figure 7.11 – Graphical representation of the pressure over time for the CO2 permeability essay. (A – feed; B – permeate).

By modifying the Equation 3.30 and making it a linear equation ($y = mx + b$) where the slope (m) match the film permeability to the test gas. In Figure 7.12 the graphic with the two terms of the equation and the tendency line is presented.

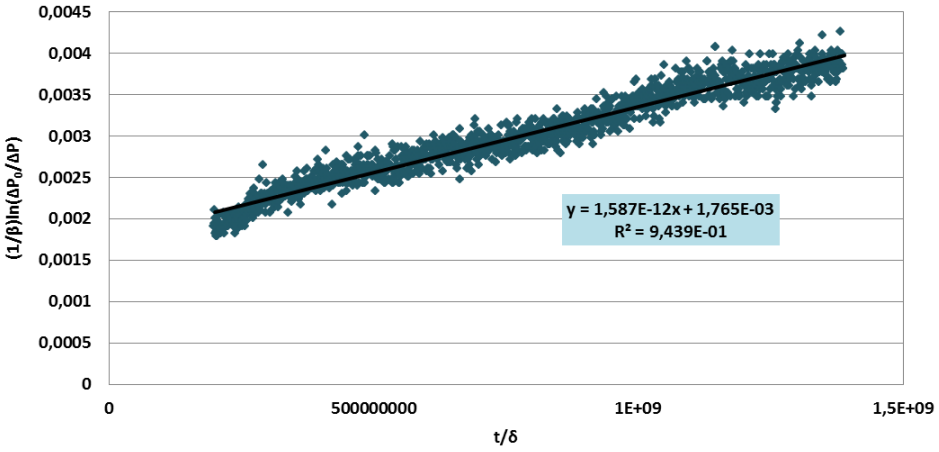

Figure 7.12 – Graphical representation of the experimental data from where the permeability is obtained.

Table 7.13 - Carbon dioxide permeability.

Film	Thickness (μm)	CO_2P (10^{-15} mol.m/m^{2}sPa)
Ch	63.30 ± 2.12	0.612 ± 0.028
Ch + 1% BW	55.40 ± 5.09	0.700 ± 0.050
Ch + 5% BW	60.00 ± 2.83	1.039 ± 0.054
Ch + 10% BW	62.70 ± 3.82	2.087 ± 0.081

ANNEX VII. POSTER

EDIBLE COATINGS BASED ON CHITOSAN-BEESWAX EMULSIONS

Sónia Marques[1], Ana R. Ferreira[1], Isabel Coelhoso[1], Isabel Sousa[2], Margarida Moldão-Martins[2], Vítor D. Alves[2]

[1]REQUIMTE/CQFB, Chemistry Department, FCT/Universidade Nova de Lisboa, 2829-516 Caparica, Portugal, imrc@fct.unl.pt.

[2]CEER-Biosystems Engineering, Institute of Agronomy, Technical University of Lisbon, Tapada da Ajuda, 1349-017 Lisbon, Portugal, vitoralves@isa.utl.pt

❖ Introduction

Nowadays, the use of minimally processed products, ready to eat, and preferably free from preservatives has increased. This has contributed for developing films with antioxidant and antimicrobial properties and with the ability to control water and permeability, flavours and solute transport. These films may be classified as active packaging structures and are one of the most promising solutions to extend food products shelf-life, being at the same time an environmentally friendly alternative to common plastic packaging.

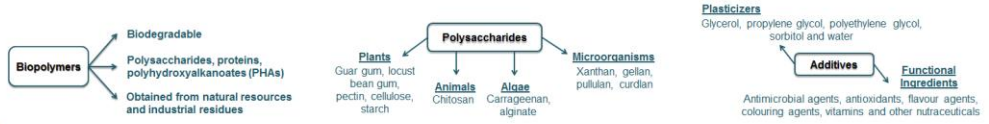

❖ Films preparation

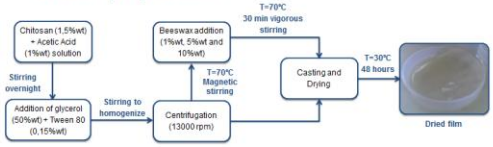

❖ Films morphology

- Flexible and transparent films
- Bended without breaking
- Thickness of 60 ± 5 µm and homogeneous films

- SEM images:

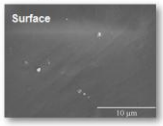

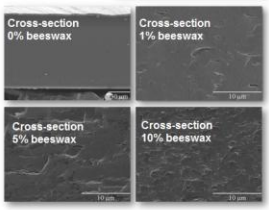

- All the surface images are alike
- In the cross-section images, with the increasing of beeswax content, more depressions and cracks were observed, without the formation of pores.

❖ Water sorption isotherms

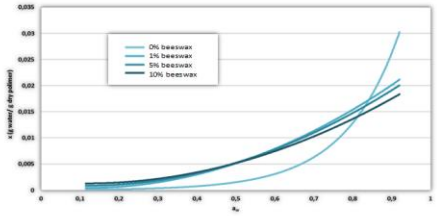

- Determined by the gravimetric method

❖ Barrier properties

- Poor water vapour barrier
- WVP decreases slightly with the increase of beeswax content

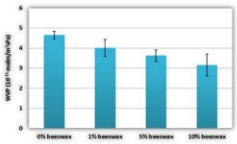

(Driving force of 80,6 – 32,4 RH%)

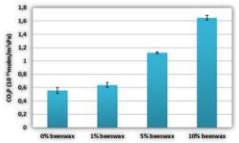

(Water content from 5 to 10 %, dry basis)

- Good CO_2 barrier
- PCO_2 increases strongly with de increase of the percentage of the incorporated beeswax

❖ Optical properties

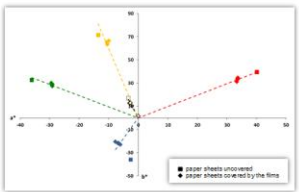

- Good transparency
- Colour alteration may still be perceived by human eye ($\Delta E_{ab} > 3$)

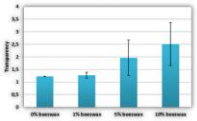

❖ Mechanical properties

- Measurements made under tensile tests
- Flexible films
- High strain at break
- Low Young modulus

Films	Stress at break (MPa)	Strain at break (%)	Young modulus (MPa)
0% beeswax	16.0 ± 2.4	48.9 ± 3.9	27.2 ± 0.9
1% beeswax	15.0 ± 2.1	37.3 ± 1.8	26.8 ± 0.4
5% beeswax	13.7 ± 0.1	42.0 ± 1.8	21.3 ± 2.4
10% beeswax	6.2 ± 1.1	29.9 ± 3.7	17.6 ± 1.2

❖ Conclusions

- All the obtained films are quite flexible and elastic, they are transparent with a slightly yellowish colour probably due to the tween 80 and beeswax addition.
- The films of chitosan and chitosan with incorporation of beeswax are all very hydrophilic and their water sorption isotherms show the same behavior (the higher water activity of the solution that the film was subjected, the greater the adsorption of water).
- The permeability to water vapour decreased about 30% with the addition of 10% (dry basis) of beeswax.
- The permeability to CO2 increased significantly with beeswax content. It may be attributed to the increase of the chitosan-beeswax matrix hydrophobic character.
- With regard to the mechanical properties, the stress at break, strain at break and Young modulus decreased with the increase of the amount of incorporated beeswax. It can be concluded that the incorporation of beeswax weakened the structure of the films, making them less resistant.

❖ Acknowledgements

- The authors would like to acknowledge FCT-MCTES, Portugal, for funding of project PTDC/AGR-ALI/114706/2009 – "New edible bioactive coatings for the improvement of food products quality".
- A. R. Ferreira also acknowledges her scholarship in the frame of this project.

❖ References

- Dutta, P.K., Tripathi, S., Mehrotra, G.K., Dutta, J. (2009). Perspectives for chitosan based antimicrobial films in food application. *Food Chemistry*. 114, 1173–1182.
- Jong-Whan Rhim & Perry K.W. Ng (2007): Natural Biopolymer-Based Nanocomposite Films for Packaging Applications, Critical Reviews in Food Science and Nutrition, 47:4, 411-433
- Alves, V.D., Costa, N., Coelhoso, I.M. (2010). Barrier properties of biodegradable composite films based on kappa-carrageenan/pectin blends and mica flakes. *Carbohydrate Polymers*. 69, 269–276.